Synthesis and reactivity of homo- and hetero-dimetallic complexes bridged by diphenyl-2-pyridylphosphine and hydrides: regioselectivity of alkyne insertion into unsaturated $M^1(\mu\text{-}PPh_2Py)(\mu\text{-}H)_2M^2$ moieties†

Yoshinori Takahashi,[a] Naoaki Murakami,[a] Ken-ichi Fujita*[a,b] and Ryohei Yamaguchi*[a]

Received 11th September 2008, Accepted 25th November 2008
First published as an Advance Article on the web 30th January 2009
DOI: 10.1039/b815890h

New homo- and hetero-dimetallic complexes bridged by diphenyl-2-pyridylphosphine and hydrides $[(Cp^*Ir)(\mu\text{-}PPh_2Py)(\mu\text{-}H)_2(MCp^*)][OTf]_n$ (**3**: M = Ir, n = 2; **4**: M = Rh, n = 2; **5**: M = Ru, n = 1) were synthesized. The reactions of **3** with terminal alkynes gave μ-vinyl complexes $[(Cp^*Ir)(\mu\text{-}PPh_2Py)(\mu\text{-}H)(\mu\text{-}C(R)=CH_2)(IrCp^*)][OTf]_2$ (**6**: R = H; **7**: R = CO_2Me; **9**: R = Ph) and $[(Cp^*Ir)(\mu\text{-}PPh_2Py)(\mu\text{-}H)(\mu\text{-}CH=CHR)(IrCp^*)][OTf]_2$ (**8**: R = $SiMe_3$; **10**: R = Ph). The reactions of **4** with alkynes gave $[(Cp^*Ir)(\mu\text{-}PPh_2Py)(\mu\text{-}H)(\mu\text{-}C(R)=CH_2)(RhCp^*)][OTf]_2$ (**11a**: R = H; **12a**: R = CO_2Me; **13a**: R = Ph), two of which are in equilibrium with $[(Cp^*Ir)(\mu\text{-}PPh_2Py)(\mu\text{-}H)(\mu\text{-}CH_2=C(CO_2Me))(RhCp^*)][OTf]_2$ (**12b**) and $[(Cp^*Ir)(\mu\text{-}PPh_2Py)(\mu\text{-}H)(\mu\text{-}CH_2=C(Ph))(RhCp^*)][OTf]_2$ (**13b**) at 50 °C, respectively. The reactions of **5** with alkynes gave $[(Cp^*Ir)(\mu\text{-}PPh_2Py)(\mu\text{-}H)(\mu\text{-}CH_2=C(R))(RuCp^*)][OTf]$ (**14b**: R = CO_2Me; **15b**: R = Ph). Plausible pathways for the insertion of alkynes to the metal–hydride bonds and the interconversion of the μ-vinyl complexes are discussed. Structures of the cationic parts of **3**, **8**, **9**, **13b**, **14b** and **15b** have been confirmed by X-ray analysis.

Introduction

Metal hydrides play important roles in a number of transition metal-catalyzed reactions such as hydrogenation, hydroformylation and the Wacker–Höchst process.[1] Especially, insertion reactions of unsaturated organic molecules into a metal–hydride bond are quite important, thus fundamental reactivities of monometallic hydrido complexes towards alkenes, alkynes, carbonyls and other unsaturated compounds have been extensively studied experimentally and theoretically.[2] In recent years, the chemistry of multimetallic complexes has been attracting much attention, because cooperative reactivity and synergistic effects of multi-metal centers in close proximity can be expected.[3,4] As for multi-metallic hydrido complexes, several coordinatively unsaturated complexes having bridging hydrides have been synthesized and their reactivity towards unsaturated organic molecules has been disclosed.[4b,5–7] For example, Riera and Ruiz reported the reactions of $[Mn_2(\mu\text{-}H)_2(CO)_6(\mu\text{-}dppm)]$ [dppm = bis(diphenylphosphino)methane] with terminal alkynes to give $[Mn_2(\mu\text{-}CR=CH_2)(\mu\text{-}H)(CO)_6(\mu\text{-}dppm)]$ (R = H, Ph) complexes *via* insertion of a carbon–carbon triple bond into a metal–hydride bond.[5b] Puddephatt has reported the reversible insertion of alkynes into $[Ru_2(\mu\text{-}H)(\mu\text{-}CO)(CO)_4(\mu\text{-}dppm)_2]^+$ to give $[Ru_2(\mu\text{-}CH=CH_2)(CO)_4(\mu\text{-}dppm)_2]^+$ and $[Ru_2(\mu\text{-}CH=CHPh)(CO)_4(\mu\text{-}dppm)_2]^+$.[5f] We have also reported the reactions of a dmpm and dihydrido-bridged diiridium complex, $[(Cp^*Ir)_2(\mu\text{-}H)_2(\mu\text{-}dmpm)]^{2+}$ [dmpm = bis(dimethylphosphino)methane, $Cp^* = \eta^5\text{-}C_5Me_5$], with alkynes to give μ-vinyl complexes $[(Cp^*Ir)_2(\mu\text{-alkenyl})(\mu\text{-}dmpm)(\mu\text{-}H)]^{2+}$.[4b] In these reactions, the regioselectivity of the alkyne insertion to give α- and β-isomers and the isomerization process of these isomers have been demonstrated (eqn (1)).

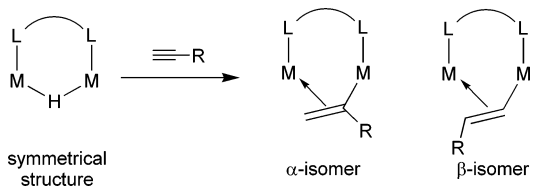

(1)

However, most of these studies have been performed using symmetrical homo-dimetallic complexes in which two metal centers are in the same environment. In view of high functionality of multimetallic complexes, it should be interesting to study the reactivity of unsymmetrical homo-dimetallic or hetero-dimetallic complexes containing the unsaturated $M^1(\mu\text{-}H)M^2$ core.[8] Additionally, it is also important to reveal the regioselectivity of the insertions into $M^1(\mu\text{-}H)M^2$ in which two metal centers are in different environments. Herein, we wish to report our studies on the alkyne insertion reactions into $L^1M^1(\mu\text{-}H)M^2L^2$, which might afford multiple isomers of μ-vinyl complexes.

We have focused on diphenyl-2-pyridylphosphine (PPh_2Py)[9] as an unsymmetrical bridging ligand, which keeps two metal centers in close proximity and provides different environments to two metal centers. In this paper, we report the synthesis of homo- and hetero-dimetallic complexes of iridium, rhodium and ruthenium bridged by PPh_2Py as well as dihydrides, and their reactivity towards alkynes. The expected eight types of isomers [four regioisomers (type **I** to **IV**) and two conformers of each] are

[a]*Graduate School of Human and Environmental Studies, Kyoto University, Sakyo-ku, Kyoto, 606-8501, Japan. E-mail: yama@kagaku.mbox.media.kyoto-u.ac.jp; Fax: +81 75 753 6634; Tel: +81 75 753 6840*
[b]*Graduate School of Global Environmental Studies, Kyoto University, Sakyo-ku, Kyoto, 606-8501, Japan. E-mail: fujitak@kagaku.mbox.media.kyoto-u.ac.jp; Fax: +81 75 753 6634; Tel: +81 75 753 6827*

† CCDC reference numbers 701920 **3-BPh_4**, 701921 **8-BPh_4**, 701922 **9-BPh_4·(C_3H_6O)**, 707683 **13b-BPh_4·(C_3H_6O)**, 701923 **14b·(C_3H_6O)** and 701924 **15b**. For crystallographic data in CIF or other electronic format see DOI: 10.1039/b815890h

shown in eqn (2). The regioselectivity of these insertion reactions and the interconversion of the μ-vinyl complexes are discussed below.

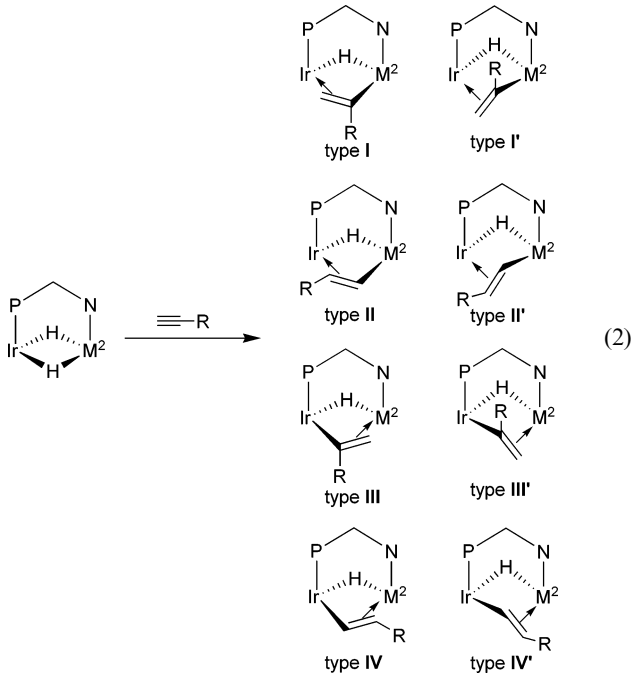

(2)

Results and discussion

Synthesis of homo- and hetero-dimetallic complexes bridged by PPh_2Py and hydrides

Although dimetallic complexes bridged by PPh_2Py are well known,[9] to the best of our knowledge, there has been no report on the complexes having hydrides as additional bridging ligands. We planned to synthesize a series of dimetallic complexes using $Cp^*Ir(PPh_2Py)(H)_2$ (**1**) as a template; *i.e.* the reaction of **1** with coodinatively unsaturated transition metal precursors $[M^2L_n]$ would afford the dimetallic complexes $Cp^*Ir(\mu\text{-}PPh_2Py)(\mu\text{-}H)_2M^2L_n$. The template **1** was prepared as follows. At first, the treatment of $[Cp^*IrCl_2]_2$ with PPh_2Py (1.1 equiv.) in THF at room temperature gave the monodentate complex $Cp^*Ir(PPh_2Py)(Cl)_2$ (**2**) in good yield (eqn (3)).[10] In the ^1H NMR of **2**, a signal due to the Cp* ligand was observed at δ 1.37 ppm as a doublet coupled to phosphorus ($J_{PH} = 2$ Hz). In the $^{31}P\{^1H\}$ NMR, a single resonance was found at δ 0.8 ppm, which was at lower field compared to the uncoordinated PPh_2Py (δ −3.4 ppm). The spectroscopic data clearly indicated that the PPh_2Py ligand was coordinated to the iridium center through the phosphorus atom as illustrated. Complex **2** was converted into the dihydrido complex **1** by reaction with lithium triethylborohydride (eqn (4)). Complex **1** was isolated in 77% yield after purification by column chromatography. In the ^1H NMR of **1**, a signal due to two hydrides was observed at δ −16.89 ppm as a doublet coupled to the phosphorus ($J_{PH} =$ 31 Hz). In the $^{31}P\{^1H\}$ NMR, a singlet resonance was observed at δ 21.1 ppm. All NMR data (^1H, $^{13}C\{^1H\}$, and $^{31}P\{^1H\}$) were consistent with the proposed structure.

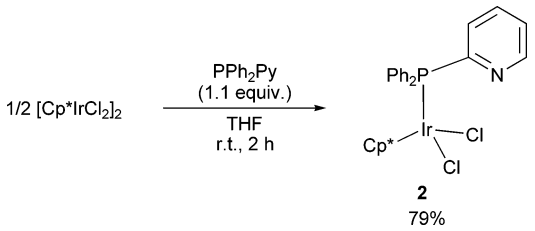

(3)

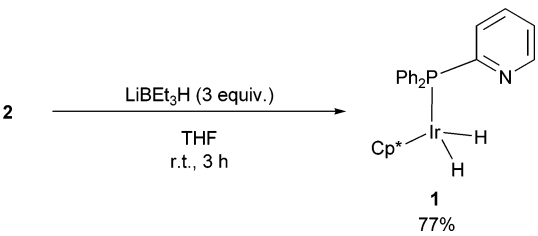

(4)

Having the template complex **1** in hand, we next carried out the synthesis of homo- and hetero-dimetallic complexes by the reaction with coordinatively unsaturated metal precursors. When an equimolar amount of $[Cp^*Ir(MeCN)_3][OTf]_2$ was added to a solution of **1** in acetone, the colour of the solution quickly turned to dark brown to give the new homo-dimetallic diiridium complex **3** in 92% yield (eqn (5)). The structure of **3** was elucidated by the spectroscopic data as well as the X-ray diffraction study of the anion-exchanged complex **3-BPh$_4$**. In the ^1H NMR spectrum of **3**, two signals due to Cp* ligands were observed non-equivalently at δ 1.92 and 1.77 ppm. The former resonance at δ 1.92 ppm was observed as a doublet coupled to phosphorus ($J_{PH} = 2$ Hz) while the latter resonance was observed at δ 1.77 ppm as a singlet, indicating that one of the Cp*Ir moieties bound to phosphorus and the other bound to nitrogen of the pyridine ring. A characteristic signal due to the bridging hydrido ligands was observed at δ −14.78 ppm as a doublet coupled to phosphorus with a relatively small coupling constants ($J_{PH} = 15$ Hz) compared to the terminal hydrides of monometallic complex **1** ($J_{PH} = 31$ Hz). Additionally, a signal due to the α-proton of the pyridine ring was observed at δ 9.66 ppm, which was shifted to lower field compared to that in **1** (δ 8.37 ppm) or **2** (δ 8.68 ppm). In the ^{31}P NMR, a singlet resonance was observed at δ 45.6 ppm. The X-ray diffraction study of **3-BPh$_4$**, which was prepared by the anion metathesis using $NaBPh_4$, was carried out to confirm the structure of the cationic part of **3**. The molecular geometry and atom numbering system are shown in Fig. 1. It is apparent that two Cp*Ir moieties are bridged by PPh_2Py. The iridium–iridium distance is 2.7122(2) Å, which is comparable to the isoelectronic complex $[(Cp^*Ir)_2(\mu\text{-dmpm})(\mu\text{-}H)_2]^{2+}$ (2.7236(8) Å).[4b] Two hydrides are located from the Fourier difference map, clearly showing that hydrides are also bridging two iridium centers.

In addition to the homo-dimetallic complex **3**, hetero-dimetallic complexes **4** and **5** were also synthesized. The treatment of **1** with $[Cp^*Rh(MeCN)_3][OTf]_2$ gave the hetero-dimetallic iridium–rhodium complex **4** in 83% isolated yield (eqn (5)). Since the NMR spectra of **4** showed broad unresolved resonance at room temperature; thus those were measured at −20 °C.[11] In the ^1H NMR, a signal due to the bridging hydrides were observed at δ −15.30 ppm as a doublet of doublets coupled to both phosphorus ($J_{PH} = 20$ Hz) and rhodium ($J_{RhH} = 20$ Hz), reflecting its core structure of P-Ir(μ-H)$_2$Rh. A characteristic signal due to the α-proton in the pyridine ring was observed at δ 9.43 ppm similar

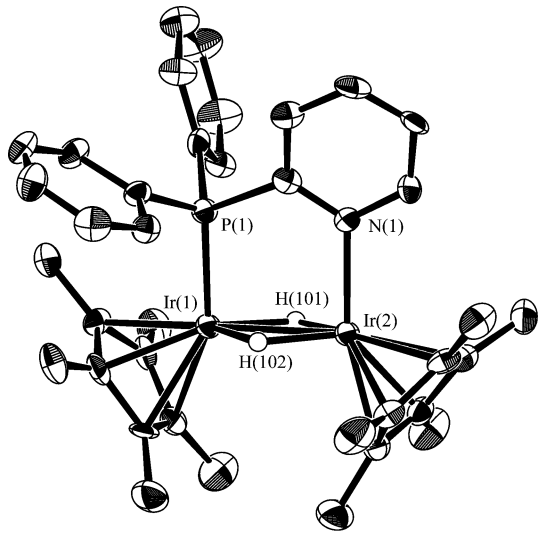

Fig. 1 ORTEP drawing of the cationic part of **3-BPh$_4$**. Counter anions and hydrogen atoms except for metal hydrides are omitted for clarity.

to that in **3**. In the $^{31}P\{^1H\}$ NMR, a signal due to phosphorus was observed at δ 26.1 ppm as a singlet, indicating that there is no bonding interaction between rhodium and phosphorus. The similar reaction of **1** with [Cp*Ru(MeCN)$_3$][OTf] gave the hetero-dimetallic iridium–ruthenium complex **5** (eqn (5)), which was relatively unstable. In the ^1H NMR of **5**, a signal due to two hydrides was observed at δ –16.13 ppm as a doublet coupled to the phosphorus (J_{PH} = 20 Hz), and another characteristic signal due to the α-proton of the pyridine ring was observed at δ 9.87 ppm. In the $^{31}P\{^1H\}$ NMR, a singlet signal was observed at δ 11.5 ppm. All NMR data (^1H, $^{13}C\{^1H\}$, and $^{31}P\{^1H\}$) were consistent with the proposed structure.

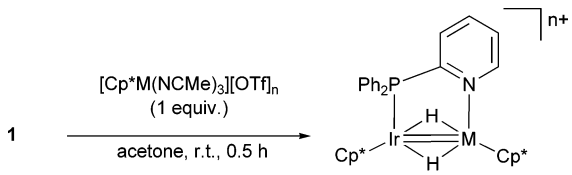

(5)

3: M = Ir, n = 2, 92%
4: M = Rh, n = 2, 83%
5: M = Ru, n = 1, 90%

Reactions of homo-dimetallic complex 3 with alkynes[12]

We have previously reported the reactions of alkynes with the dmpm and dihydrido-bridged symmetrical diiridium complex, $[(Cp^*Ir)_2(\mu\text{-}H)_2(\mu\text{-dmpm})]^{2+}$, which resulted in the formation of a mixture of α- and β-isomers of μ-vinyl complexes.[4b] Having the new diiridium complex **3** bridged by PPh_2Py and dihydride in hand, we examined the reactions with terminal alkynes to reveal the regioselectivity of the insertion.[13] The reaction of **3** with ethyne at room temperature gave the μ-vinyl complex **6** quantitatively, and **6** was isolated in 84% yield (eqn (6)). Complex **6** was the sole product, and the formation of other isomers was not observed. In the ^1H NMR of **6**, three signals due to μ-vinyl ligand were observed at δ 7.35, 4.69 and 2.81 ppm (Table 1). These signals could be assigned as the α-vinyl proton, the *trans* β-vinyl proton and the *cis* β-vinyl proton, respectively. The relatively large vicinal coupling constant between the *cis* β-vinyl proton and phosphorus ($^3J_{PH}$ = 14 Hz) indicates the *syn* conformation around the Ir–C$^\beta$ bond.[14] In the $^{13}C\{^1H\}$ NMR, two signals due to the μ-vinyl carbons were observed at δ 119.5 (C$^\alpha$) and 54.2 ppm (C$^\beta$). All the NMR data of **6** are consistent with the proposed structure and analogous to those of the μ-vinyl complex $[(Cp^*Ir)_2(\mu\text{-dmpm})(\mu_2,\eta^1,\eta^2\text{-}CH{=}CH_2)(\mu\text{-}H)]^{2+}$, which we have previously reported.[4b] Next, the reaction of **3** with methyl propiolate gave a similar μ-vinyl complex **7** in 69% yield (eqn (6)). The structure of **7** can be described as the α-isomer of the type **I** (see, eqn (2)). Complex **7** was characterized by NMR spectroscopy. In the ^1H NMR, two signals due to the μ-vinyl protons were observed at δ 4.84 (*trans* β-vinyl proton) and 2.42 ppm (*cis* β-vinyl proton). In the $^{13}C\{^1H\}$ NMR, signals due to the μ-vinyl carbons were observed at δ 120.4 (C$^\alpha$) and 46.2 ppm (C$^\beta$). The signal patterns of the NMR spectra of **7** were closely similar to those of **6** except for the α-vinyl proton in **6**.

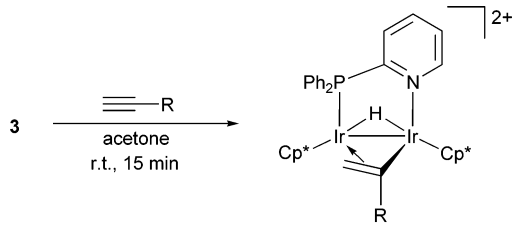

(6)

6 R = H (84%)
7 R = CO_2Me (69%)

We next examined the reaction of **3** with an alkyne with a bulky substituent. When **3** was treated with trimethylsilylacetylene at room temperature for 15 min, the β-isomer of the μ-vinyl complex **8** having the type **IV′** structure was obtained in 95% yield with a small amount of contaminant (< 10%) (eqn (7)).[15] The structure of **8** was elucidated by NMR analysis and X-ray diffraction study of the anion exchanged complex **8-BPh$_4$**. In the ^1H NMR of **8**, two doublets due to the μ-vinyl protons were observed at δ 8.35 (α-vinyl proton) and 5.29 ppm (β-vinyl proton). Relatively large coupling constants between these vinyl protons (J_{HH} = 17 Hz) indicated its *trans* configuration. In the $^{13}C\{^1H\}$ NMR, signals due to the μ-vinyl carbons were observed at δ 145.9 ppm as a doublet (C$^\alpha$, J_{PC} = 4 Hz) and 99.8 ppm as a doublet (C$^\beta$, J_{PC} = 4 Hz). The structure of the cationic part of **8** was further confirmed by X-ray crystallography of **8-BPh$_4$** (Fig. 2 and Table 2). The iridium–iridium distance is 2.8680(6) Å, which is comparable to that of $[(Cp^*Ir)_2(\mu\text{-dmpm})(\mu\text{-}H)(\mu\text{-}CH{=}CHPh)]^{2+}$.[4b] Trimethylsilyl group is directed to outside away from Cp* ligands and occupies the void space in front of the pyridine ring because of its steric repulsion.

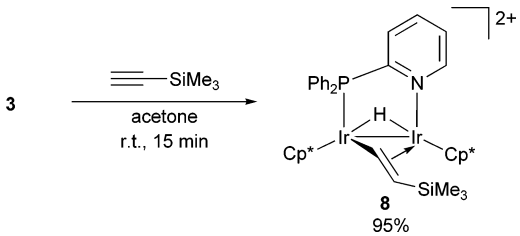

(7)

8
95%

The reaction of **3** with phenylacetylene gave a mixture of isomers of μ-vinyl complexes. The ratio of products was determined by NMR of a crude mixture [**9** (34%) and **10** (43%), along with an unidentified minor product (eqn (8))].[16] By column chromatography, pure **9** and a mixture of **10** and the unidentified isomer were obtained. The structure of **9** was determined by

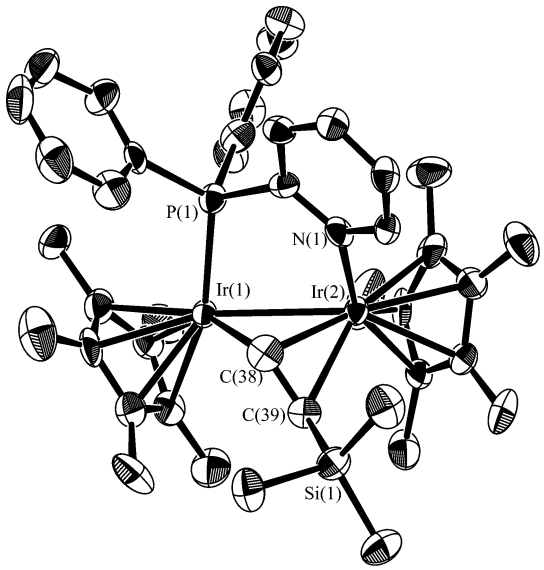

Fig. 2 ORTEP drawing of cationic part of **8-BPh$_4$**. Counter anions and hydrogen atoms are omitted for clarity.

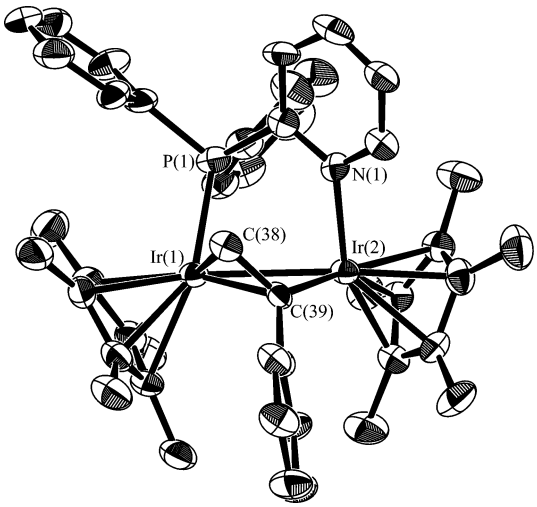

Fig. 3 ORTEP drawing of the cationic part of **9-BPh$_4$**. Counter anions and hydrogen atoms are omitted for clarity. In the unit cell, there are two independent molecules, which are very similar to each other.

NMR spectroscopy and X-ray diffraction. In the ^{1}H NMR of **9**, characteristic signals due to the μ-vinyl protons were observed at δ 4.86 and 2.65 ppm. The signal at δ 2.65 ppm was observed as a doublet of doublets coupled to phosphorus (J_{PH} = 16 Hz) and to geminal proton (J_{HH} = 3 Hz) at δ 4.86 ppm. In the ^{13}C{^{1}H} NMR spectrum, a signal due to the μ-vinyl carbon bound to iridium (C$^\alpha$) was observed at δ 146.6 ppm, and a signal due to another μ-vinyl carbon (C$^\beta$) was observed at δ 45.6 ppm. The structure of the cationic part of **9** was confirmed by X-ray analysis of the anion exchanged complex **9-BPh$_4$** (Fig. 3). It is apparent that the structure of **9-BPh$_4$** can be described as the type **I**. The carbon–carbon double bond (C(38)–C(39)) coordinates to the iridium center (Ir(1)) bound to phosphorus, and the α-carbon is σ-bonded to the iridium center (Ir(2)) bound to nitrogen. The phenyl group on the μ-vinyl moiety is directed to below the plane defined by Ir(1)–C(39)–Ir(2). In this geometry, the *cis* β-vinylic proton necessarily adopt *syn* conformation relative to phosphorus atom, supporting their spin coupling constants observed in NMR analysis. Complex **10** was characterized by NMR analysis. In the ^{1}H NMR of **10**, two signals due to the μ-vinyl protons were observed as doublets coupled to each other at δ 8.19 and 6.09 ppm, respectively. In the ^{13}C{^{1}H} NMR, signals due to the μ-vinyl carbons were observed at δ 140.9 (C$^\alpha$) and 106.5 ppm (C$^\beta$). These signal patterns of the μ-vinyl protons and carbons of **10** were very similar to those of TMS analogue **8**, supporting its structure of the type **IV′**.

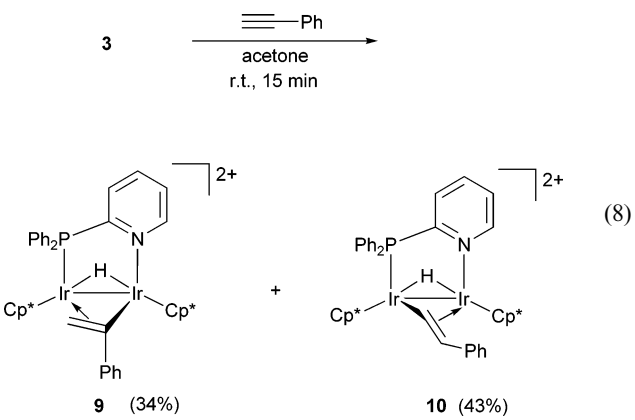

(8)

Reactivities of hetero-dimetallic complexes toward alkynes

We next examined the reactions of hetero-dimetallic complex **4** with ethyne, methyl propiolate, and phenylacetylene (eqn (9)). Products **11a–13a** were isolated in good yields, and their structures were determined by NMR spectroscopy. The reaction of **4** with ethyne gave **11a** selectively, in which the μ-vinyl ligand is σ-bonded to the rhodium center and π-coordinated to the iridium center (the type **I**). In the ^{1}H NMR of **11a**, signals due to the μ-vinyl protons were observed at δ 7.47 (α-vinyl proton), 4.28 (*trans* β-vinyl proton) and 3.10 ppm (*cis* β-vinyl proton) similar to those of **6**. In the ^{13}C{^{1}H} NMR spectrum, a characteristic signal for the α-carbon of the μ-vinyl ligand was observed in relatively lower field at δ 142.3 ppm as a doublet coupled to rhodium (J_{RhC} = 28 Hz), and a signal for the β-carbon was observed at δ 55.7 ppm as a singlet. The NMR data strongly suggests that the μ-vinyl moiety is σ-bonded to the rhodium center. The reaction of **4** with methyl propiolate and phenylacetylene gave **12a** and **13a**, respectively (eqn (9)). These products were also characterized to be α-isomers of the type **I** by NMR spectroscopy. In the ^{1}H NMR of **12a**, a signal due to the *trans* β-vinyl proton was observed at δ 4.15 ppm as a broad singlet and a signal due to the *cis* β-vinyl proton was observed at δ 2.64 ppm as a doublet of doublets coupled to phosphorus (J_{PH} = 15 Hz) and geminal proton (J_{HH} = 2 Hz). In the ^{13}C{^{1}H} spectrum, signals for the μ-vinyl carbons were observed at δ 137.9 ppm (C$^\alpha$) as a doublet (J_{RhC} = 26 Hz) and at δ 46.6 ppm (C$^\beta$) as a singlet. Although the signal patterns in ^{1}H and ^{13}C{^{1}H} NMR of **12a** were similar to those of diiridium analogue **7**, the signal for the α-carbon in **12a** shifted to the lower field. In the ^{1}H and ^{13}C{^{1}H} NMR spectra of **13a**, the signal patterns for the μ-vinyl moiety were closely similar to those of **9** except for the coupling between rhodium and C$^\alpha$.

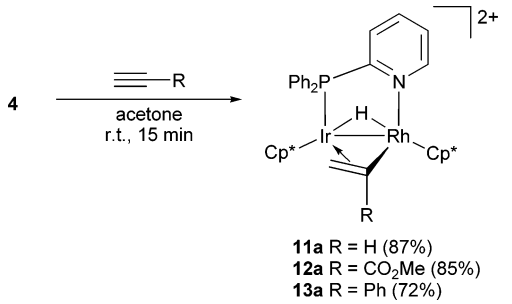

(9)

11a R = H (87%)
12a R = CO_2Me (85%)
13a R = Ph (72%)

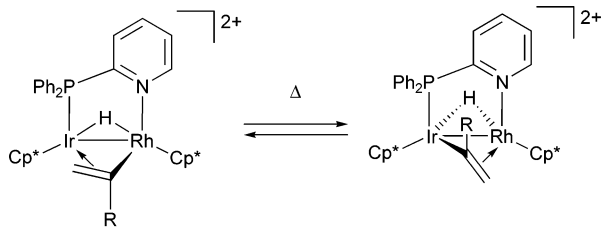

(10)

after heating at 50 °C for 5 h **12a/12b** = 1.5
13a/13b = 0.11

Interestingly, **12a** and **13a** were slowly converted into the other isomers **12b** and **13b**, respectively (eqn (10)). Heating a solution of **12a** in acetone at 50 °C for 5 h gave an equilibrium mixture of **12a** and **12b** in a ratio of 1.5. The structure of **12b** was determined to be as illustrated in eqn (10) by NMR analysis. In the ^{1}H NMR of **12b**, two singlets due to the vinylic protons were observed at δ 7.21 and 5.04 ppm, and a pseudo triplet due to the bridging hydride coupled to both phosphorus and rhodium was observed at δ −17.07 ppm (J = 22 Hz). In the ^{13}C{^{1}H} NMR, the μ-vinyl carbons were observed at δ 146.9 (C^{α}) and 98.7 ppm (C^{β}). These signal patterns were different from those of type **I** isomers (**6**, **7**, **9** and **11a–13a**) or type **IV′** isomers (**8** and **10**). We characterized this complex as the type **III′** isomer. Similarly, heating a solution of **13a** in acetone resulted in an equilibrium of **13a** (the type **I**) and **13b** (the type **III′**) in a ratio of 0.11. In the ^{1}H NMR of **13b**, signals due to μ-vinyl protons were observed at δ 6.61 and 5.01 ppm. In the ^{13}C{^{1}H} NMR, signals due to μ-vinyl carbons were observed at δ 171.1 (C^{α}) and 86.0 ppm (C^{β}). The structure of the cationic part of **13b** was confirmed by X-ray diffraction study of the anion exchanged complex **13b-BPh$_4$** (Fig. 4). It is apparent that the carbon–carbon double bond coordinates to the rhodium center and the α-carbon was σ-bonded to the iridium center. It should be noted that phenyl group bound to C(39) atom is directed upward from the plane defined by Ir(1)–C(39)–Rh(1) in contrast to **9-BPh$_4$**, in which phenyl group is directed downward. Thus, we characterized **13b** as the type **III′** isomer. In contrast to these results, **11a** remained unchanged after heating the solution up to 80 °C for 12 h.

Finally, we investigated the reactions of hetero-dimetallic complex **5** with alkynes (eqn (11)). Because of the thermal instability of **5**, the reactions of **5** with alkynes were carried out immediately after **5** was generated *in situ*. The treatment of **1** with [Cp*Ru(NCMe)$_3$][OTf] in acetone gave a green solution of **5**, then methyl propiolate was added, and the mixture was stirred for 15 min. By this procedure, the complex **14b**, which is an α-isomer of the type **III′** (σ-bonded to the iridium center and π-coordinated to the ruthenium center), was obtained in 64% yield. The structure of **14b** was determined by NMR spectroscopy and X-ray diffraction study. In the ^{1}H NMR, two singlets due to the vinylic protons were observed at δ 5.99 and 3.85 ppm. A signal due to the bridging hydride was observed at δ −19.94 ppm coupled to phosphorus (J_{PH} = 28 Hz). In the ^{13}C{^{1}H} NMR, signals due to the μ-vinyl carbons were observed at δ 115.6 ppm (C^{α}) as a doublet and 77.5 ppm (C^{β}) as a singlet. These signal patterns are relatively similar to those of the type **III′** isomers such as **12b** and **13b**. The structure of **14b** was confirmed by X-ray analysis (Fig. 5). The carbon–carbon double bond coordinates to the ruthenium center and the α-carbon was σ-bonded to the iridium center and the methoxycarbonyl group on C(39) atom is directed upward from the plane defined by Ir(1)–C(39)–Ru(1). The reaction of **5** with phenylacetylene also gave the complex **15b** having the type **III′** structure in 96% yield. In the ^{1}H NMR of **15b**, signals due to the μ-vinyl protons were observed at δ 5.39 and 4.18 ppm. In the ^{13}C{^{1}H} NMR, signals due to the μ-vinyl carbons were observed at δ 133.9 ppm as a doublet (C^{α}) and 75.6 ppm as a singlet (C^{β}).

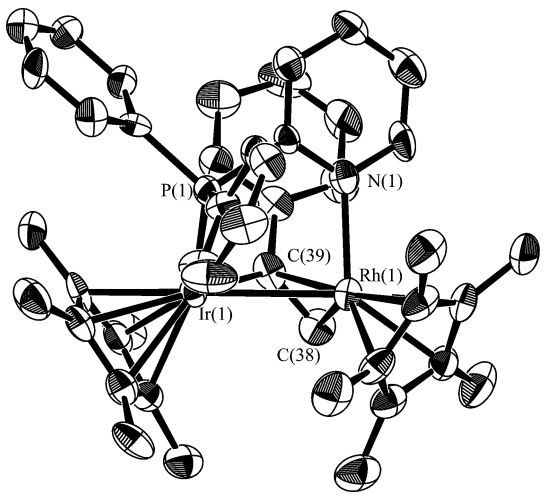

Fig. 4 ORTEP drawing of cationic part of **13b-BPh$_4$**. Counter anions and hydrogen atoms are omitted for clarity.

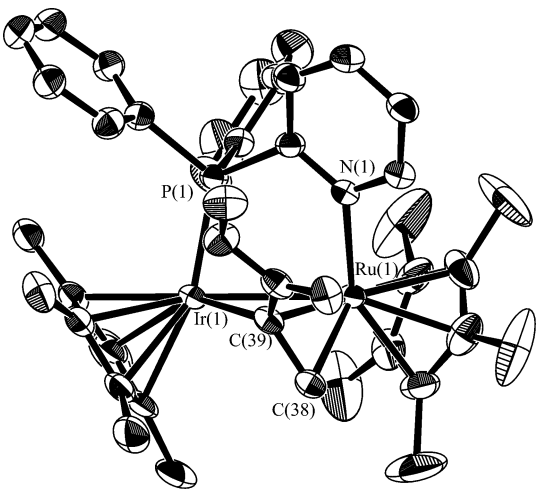

Fig. 5 ORTEP drawing of cationic part of **14b**. Counter anions and hydrogen atoms are omitted for clarity. In the unit cell, there are two independent molecules, which are very similar to each other.

Finally, X-ray diffraction revealed the structure of **15b** (Fig. 6). It is apparent that the μ-vinyl ligand is σ-bonded to the iridium center and π-coordinated to the ruthenium center in a similar manner to the case of **14b**.

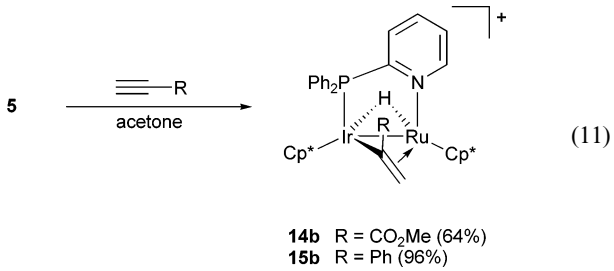

(11)

14b R = CO_2Me (64%)
15b R = Ph (96%)

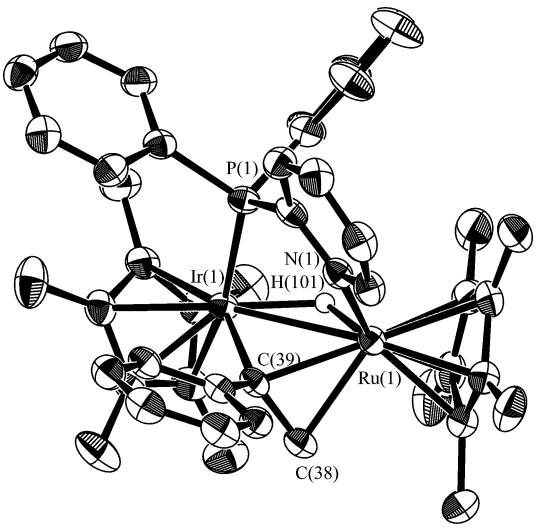

Fig. 6 ORTEP drawing of cationic part of **15b**. Counter anions and hydrogen atoms except for metal hydride are omitted for clarity.

Considerations on the regioselectivity in alkyne insertions and the isomerization of the μ-vinyl complexes

From the results shown above, we propose the possible pathways for the insertion of alkynes to the diiridium complex **3** and the iridium–rhodium complex **4** (Scheme 1). The selective formation of the type **I** complexes (**6** and **7**) in the reaction of **3** with less bulky alkynes such as ethyne or methyl propiolate indicates that these reactions would start with coordination of carbon–carbon triple bond to the iridium center bound to phosphorus to afford **A** and the subsequent hydroiridation could lead to the type **I** products (Scheme 1, the left line).[17] On the other hand, in the reaction with trimethylsilylacetylene, sterically demanding trimethylsilyl group could prevent coordination to the iridium center bound to phosphorus. Instead, trimethylsilylacetylene would coordinate to the less hindered iridium center having pyridine ligand to afford **B**, in which bulky trimethylsilyl group is directed away from the diiridium center (Scheme 1, the right line). Then, hydroiridation would occur to give the type **IV′** complex **8**.

The regioselectivity in the reactions of the hetero-dimetallic complex **4** can be also rationalized as follows. The selective formation of the type **I** complexes (**12a** and **13a**) in the reactions of **4** with alkynes and their isomerization to the type **III′** complexes (**12b** and **13b**) suggest that the type **I** complexes are the kinetic

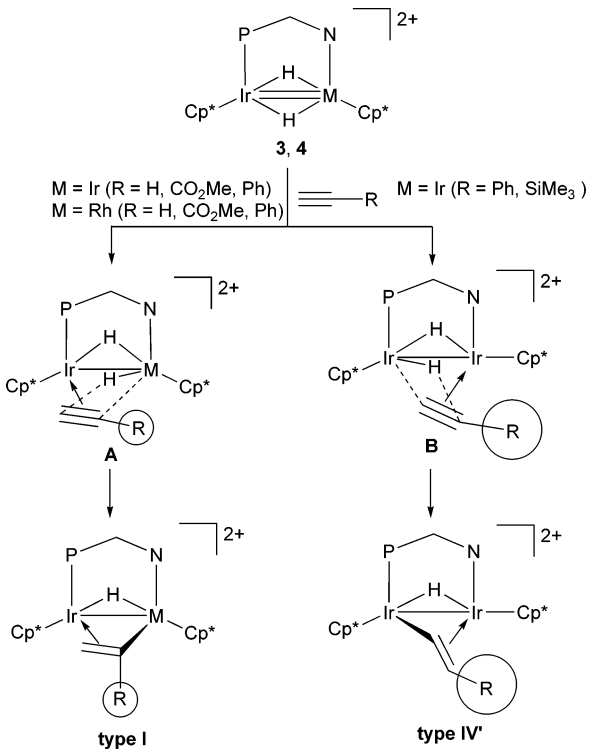

Scheme 1 Plausible pathways for the insertion of alkynes to the dimetallic complexes **3** and **4**

products. As illustrated in Scheme 1, the reaction of **4** with alkynes would start with coordination of alkynes to the iridium center to afford **A** in the similar manner to the case of homo-dimetallic complex **3**. Then, hydrometallation would occur to give a μ-vinyl complex of the type **I** as a kinetic product. To support the insertion pathway described above, we have carried out the isotope-labelling experiments. The reaction of **4** with phenylacetylene-d_1 (PhCCD) gave the deuterated product **13a**-d_1, in which the *trans* β-vinylic proton was selectively dueterated (> 99% D).[18] This result strongly suggests that *cis* hydrorhodation to the carbon–carbon triple bond coordinated to the iridium center has occurred.

The reaction of the iridium–rhodium complex **4** with phenylacetylene gave the type **I** complex **13a** exclusively, while a similar reaction with the iridium–iridium complex **3** gave the mixture of type **I** (**9**) and type **IV′** (**10**) complexes. These results can be explained as follows. In the case of **3**, both of the pathways in Scheme 1 would be operative because phenylacetylene is moderately sterically demanding. On the other hand, in the case of **4**, phenylacetylene would be selectively coordinated to the iridium center in the first step to afford **A**, because of the greater ability of iridium for π-back bonding compared to that of rhodium.[19] Additionally, the hydrorhodation in **A** would be faster than the hydroiridation in **B**.[20] Thus, the pathway through **A** would be predominant in the reaction of **4** with phenylacetylene.

As shown in eqn (10), **12a**/**12b** and **13a**/**13b** were in equilibrium at 50 °C. Very recently, Ruiz *et al.* reported the fast dynamic fluxional process accompanied by the rotational isomerization of a μ-vinyl moiety in $[Mo_2Cp_2\{\mu,\eta^1,\eta^2\text{-}C(CO_2Me)=CH_2\}(\mu\text{-}PCy_2)(CO)_2]$.[5h] The interconversion processes we show here would be closely analogous to that reported by Ruiz *et al.* As illustrated in Scheme 2, **12a** or **13a** would be converted to a key intermediate

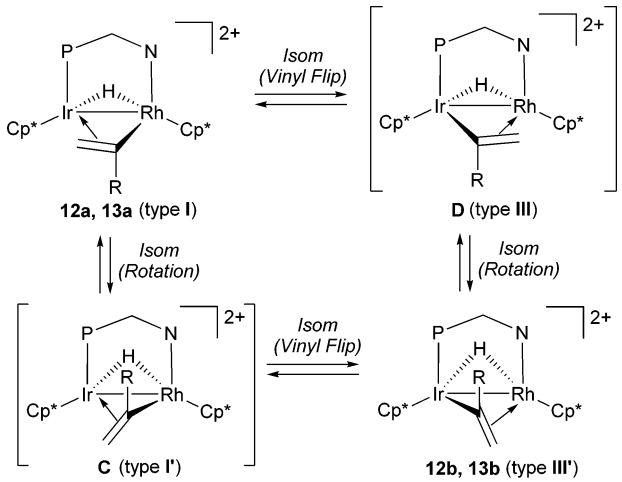

Scheme 2 Plausible pathways for the isomerization of the μ-vinyl complexes.

C (type **I′**) through rotational isomerization of the terminal CH_2 group from above to below.[21] Then, **C** would be converted to **12b** or **13b** *via* a flip of the μ-vinyl ligand (vinyl flip isomerization), which is a well-known process in dimetallic μ-vinyl complexes (this process is called "windshield wiper movement").[22] Since no equilibrium was observed in the case of **11a** that has the least hindered substituent (R = H), the elimination of the π-coordinated vinyl moiety from the left iridium center might induce the above isomerization process. Thus, the steric repulsion of substituent (R = CO_2Me or Ph) would cause the elimination of the π-coordinated vinyl moiety in **12a** or **13a** followed by the rotation around the metal–carbon bond to give **C**. Then, the subsequent vinyl flip isomerization occurs to afford **12b** or **13b**. Since the vinyl flip isomerization is generally known to proceed fast, another possible path through an intermediate **D** (type **III**) to **12b** or **13b**, in which the vinyl flip isomerization precedes to the rotational isomerization, could not be ruled out.

In the reactions of **5** with alkynes, the type **III′** complexes (**14b** and **15b**, eqn (11)) was selectively isolated as a single product. We carefully traced the reaction of **5** with methyl propiolate at −20 °C by ^{1}H and ^{31}P{^{1}H} NMR, and detected an unstable species at the initial stage (after 5 min) of the reaction.[23] Thus, it is highly probable that **14b** and **15b** would be also formed through the similar pathways as those for **12b** and **13b** (*i.e.* the initial formation of the type **I** intermediate and the subsequent isomerization to the type **III′** product).[24]

Conclusion

We have synthesized new dihydrido-bridged homo- and hetero-dimetallic complexes using the PPh_2Py ligand as an unsymmetrical bridging ligand. The reactions of the homo-dimetallic complex **3** with less hindered alkynes resulted in the selective formation of type **I** isomers, while much sterically hindered trimethylsilylacetylene gave the type **IV′** isomer. The reaction of **3** with moderately hindered phenylacetylene gave a mixture of type **I** and type **IV′** isomers, supporting that the regioselectivity would be mainly dependent on the steric repulsion between the substituents on alkynes and the dimetallic core. The reactions of the iridium–rhodium complex **4** with alkynes afforded the type **I** isomers exclusively as kinetic products. Rhodium-containing μ-vinyl complexes were in equilibrium between the type **I** and the type **III′** isomers at 50 °C. This isomerization would proceed *via* the elimination of the π-coordinated vinyl moiety followed by metal–carbon bond rotation and the subsequent vinyl flip isomerization. In the reactions of the iridium–ruthenium complex **5**, the type **III′** isomers were obtained selectively. It should be noted that one of the metal centers (left iridium in many cases) would provide a binding site for alkynes and the other metal center could work for hydrometallation to the carbon–carbon triple bond, suggesting the cooperative reactivity and the synergistic effect of multi-metal centers.[12]

Experimental

General

All reactions and manipulations were carried out under an atmosphere of argon by means of standard Schlenk techniques. ^{1}H, ^{13}C{^{1}H} and ^{31}P{^{1}H} NMR spectra were recorded on JEOL A-500 and EX-270 spectrometers. ^{31}P{^{1}H} NMR were referenced to an 85% H_3PO_4 external standard. Melting points were determined on a Yanagimoto micro melting point apparatus. Elemental analyses were carried out at the Microanalysis Center of Kyoto University.

Materials

Solvents were dried by using standard procedures and distilled prior to use. $[Cp^*IrCl_2]_2$,[25] $[Cp^*Ir(NCMe)_3][OTf]_2$,[25] $[Cp^*Rh(NCMe)_3][OTf]_2$[25] and $[Cp^*Ru(NCMe)_3][OTf]$[26] were prepared by literature methods. Chromatography was carried out by using silica-gel (Wako gel C-200) or activated alumina (Wako, 200 mesh). Other reagents were used as obtained from commercial source.

Preparation of $[Cp^*Ir(PPh_2Py)Cl_2]$ (2). During the course of the present study, Govindaswamy *et al.* reported the preparation of **2** by the reaction of $[Cp^*IrCl_2]_2$ with diphenyl-2-pyridylphosphine using dichloromethane as a solvent.[10] We have also prepared **2** using THF as a solvent. In a two-necked 50 mL flask, $[Cp^*IrCl_2]_2$ (806 mg, 1.01 mmol) and diphenyl-2-pyridylphosphine (588 mg, 2.22 mmol) were placed. After addition of THF (10 mL), the colour of the mixture turned to orange within a few minutes. Vigorous stirring for over 2 h resulted in the precipitation of an orange powder. The orange powder was filtered and washed with ether to give the light-yellow powder **2** (1.04 g, 79%). **2**: ^{1}H NMR (500.00 MHz, $CDCl_3$) δ/ppm: 8.68 (1H, m, aromatic), 7.90 (4H, m, aromatic), 7.74 (1H, br, aromatic), 7.55 (1H, m, aromatic), 7.38–7.35 (4H, m, aromatic), 7.19 (1H, m, aromatic), 1.37 (15H, d, J = 2 Hz, Cp*). ^{13}C{^{1}H} NMR (125.65 MHz, $CDCl_3$) δ/ppm: 157.5 (d, J = 78 Hz, aromatic), 148.4 (d, J = 16 Hz, aromatic), 135.2 (d, J = 9 Hz, aromatic), 135.1 (d, J = 8 Hz, aromatic), 131.8 (d, J = 54 Hz, aromatic), 131.5 (d, J = 22 Hz, aromatic), 130.2 (d, J = 6 Hz, aromatic), 127.5 (d, J = 10 Hz, aromatic), 123.7 (d, J = 2 Hz, aromatic), 92.9 (d, J = 3 Hz, C_5Me_5), 8.1 (s, C_5Me_5). ^{31}P{^{1}H} NMR (202.35 MHz, $CDCl_3$) δ/ppm: 0.8 (br, s) (literature −10.6).[10]

Preparation of $[Cp^*Ir(PPh_2Py)H_2]$ (1). To a suspension of **2** (2.04 g, 3.08 mmol) in THF (30 mL) in a two-necked 100 mL

Table 1 NMR spectral data of μ-vinyl ligands on compounds **6–15**

Compound	δ_H/ppm	δ_C/ppm	δ_P/ppm
6 (Type **I**)	7.35 (1H, ddd, J_{PH} = 2 Hz, J_{HH} = 12 Hz, 8 Hz, Ir–CH), 4.69 (1H, dd, J_{HH} = 8 Hz, 2 Hz, C=C*H*H), 2.81 (1H, ddd, J_{PH} = 14 Hz, J_{HH} = 12 Hz, 2 Hz, C=CH*H*)	119.5 (s, Ir–*C*H=), 54.2 (s, C=*C*H_2)	19.7 (s)
7 (Type **I**)	4.84 (1H, d, J_{HH} = 3 Hz, C=C*H*H), 2.42 (1H, dd, J_{PH} = 16 Hz, J_{HH} = 3 Hz, C=CH*H*)	120.4 (s, Ir–*C*(CO_2Me)=), 46.2 (s, C=*C*H_2)	20.7 (s)
8 (Type **IV′**)	8.35 (1H, d, J_{HH} = 17 Hz, Ir-C*H*), 5.29 (1H, d, J_{HH} = 17 Hz, C=C*H*)	145.9 (d, J_{PC} = 4 Hz, Ir–*C*H=), 99.8 (d, J_{PC} = 4 Hz, CH=*C*H–)	30.3 (s)
9 (Type **I**)	4.86 (1H, d, J_{HH} = 3 Hz, C=C*H*H), 2.65 (1H, dd, J_{PH} = 16 Hz, J_{HH} = 3 Hz, C=CH*H*)	146.6 (s, Ir–*C*(Ph)=), 45.6 (s, C=*C*H_2)	21.4 (s)
10 (Type **IV′**)	8.19 (1H, J_{HH} = 14 Hz, Ir–C*H*=), 6.09 (1H, d, J_{HH} = 14 Hz, C=C*H*)	140.9 (d, J_{PC} = 5 Hz, Ir–*C*H=), 106.5 (d, J_{PC} = 3 Hz, CH=*C*H–)	30.0 (s)
11a (Type **I**)	7.47 (1H, m, Rh–CH), 4.28 (1H, dd, J_{HH} = 7 Hz, 2 Hz, C=C*H*H), 3.10 (1H, ddd, J_{PH} = 13 Hz, J_{HH} = 12 Hz, 2 Hz, C=CH*H*)	142.3 (d, J_{RhC} = 28 Hz, Rh–*C*H=), 55.7 (s, CH=*C*H_2)	16.7 (s)
12a (Type **I**)	4.15 (1H, br, C=C*H*H), 2.64 (1H, dd, J_{PH} = 15 Hz, J_{HH} = 2 Hz, C=CH*H*)	137.9 (d, J_{RhC} = 26 Hz, Rh–C(CO_2Me)=), 46.6 (s, C=*C*H_2)	15.8 (s)
13a (Type **I**)	4.15 (1H, d, J_{HH} = 4 Hz, C=C*H*H), 2.74 (1H, dd, J_{PH} = 16 Hz, J_{HH} = 4 Hz, C=CH*H*)	164.7 (d, J_{RhC} = 23 Hz, Rh–*C*(Ph)=), 45.8 (s, C=*C*H_2)	16.8 (s)
12b (Type **III′**)	7.21 (1H, s, C=C*H*H), 5.04 (1H, s, C=CH*H*)	146.9 (m, Ir–*C*(CO_2Me)=), 98.7 (s, C=*C*H_2)	18.5 (s)
13b (Type **III′**)	6.61 (1H, s, C=C*H*H), 5.01 (1H, s, C=CH*H*)	171.1 (brs, Ir–*C*(Ph)=), 86.0 (d, J = 5 Hz, C=*C*H_2)	15.3 (s)
14b (Type **III′**)	5.99 (1H, s, C=C*H*H), 3.85 (1H, s, C=CH*H*)	115.6 (d, J = 6 Hz, Ir–*C*(CO_2Me)=), 77.5 (s, C=*C*H_2)	12.9 (s)
15b (Type **III′**)	5.39 (1H, s, C=C*H*H), 4.18 (1H, s, C=CH*H*)	133.9 (d, J = 10 Hz, Ir–*C*(Ph)=), 75.6 (s, C=*C*H_2)	9.4 (s)

Table 2 Selected bond lengths and angles in **3-BPh$_4$**, **8-BPh$_4$**, **9-BPh$_4$·(C_3H_6O)**, **13b-BPh$_4$·(C_3H_6O)**, **14b·(C_3H_6O)** and **15b**

	3-BPh$_4$ (M = Ir(2))	**8**-BPh$_4$ (M = Ir(2))	**9**-BPh$_4$·(C_3H_6O) (M = Ir(2))	**13b**-BPh$_4$·(C_3H_6O) (M = Rh(1))	**14b**·(C_3H_6O) (M = Ru(1))	**15b** (M = Ru(1))
Bond lengths/Å						
Ir(1)–M	2.7122(2)	2.8680(6)	2.8877(3), 2.9040(3)	2.9001(7)	2.9318(4), 2.9402(4)	2.9422(3)
Ir(1)–P(1)	2.2436(12)	2.2645(18)	2.303 (2), 2.3002(18)	2.2768(19)	2.2366(13), 2.2384(14)	2.2484(11)
M–N(1)	2.157(3)	2.169(6)	2.125(5), 2.126(6)	2.180(6)	2.180(4), 2,175(4)	2.147(3)
Ir(1)–C(38)	—	2.058(8)	2.191(6), 2.192(7)	—	—	—
Ir(1)–C(39)	—	—	2.307(5), 2.288(5)	2.042(8)	2.083(4), 2.083(4)	2.070(4)
M–C(38)	—	2.178(8)	—	2.269(8)	2.220(5), 2.204(5)	2.206(4)
M–C(39)	—	2.373(7)	2.033(8), 2.020(8)	2.316(8)	2.181(5), 2.175(5)	2.213(4)
C(38)–C(39)	—	1.331(11)	1.445(10), 1.426(11)	1.410(11)	1.402(7), 1.397(8)	1.402(7)
C(39)–C(40)	—	—	1.486(11), 1.501(11)	1.509(12)	1.488(7), 1.485(7)	1.495(6)
Bond angles/°						
M–Ir(1)–P(1)	88.95(3)	82.36(4)	79.72(4), 78.92(4)	80.20(4)	79.51(3), 79.38(3)	79.24(3)
Ir(1)–M–N(1)	91.26(10)	88.78(15)	86.52(12), 86.91(13)	87.48(16)	86.74(10), 86.70(10)	87.62(11)
P(1)–C(21)–N(1)	117.5(3)	118.9(5)	116.0(5), 115.4(5)	116.2(5)	114.6(3), 114.7(3)	115.2(3)

flask, 1M LiBEt$_3$H in THF solution (9.2 mL, 9.2 mmol) was added. After stirring for 3 h at room temperature, the resulting solution was passed through an alumina short column. Following chromatography (alumina, eluent: toluene) gave **1** as a colourless solid (1.40 g, 2.36 mmol, 77%). **1**: ^{1}H NMR (500.00 MHz, C_6D_6) δ/ppm: 8.37 (1H, m, aromatic), 8.11 (1H, m, aromatic), 7.95–7.91 (4H, m, aromatic), 7.13–7.10 (4H, m, aromatic), 7.03–6.95 (3H, m, aromatic), 6.41 (1H, m, aromatic), 1.94 (15H, s, Cp*), –16.89 (2H, d, J = 31 Hz, Ir–H). ^{13}C{^{1}H} NMR (125.65 MHz, C_6D_6) δ/ppm: 163.7 (d, J = 74 Hz, aromatic), 148.7 (d, J = 13 Hz, aromatic), 138.13 (d, J = 54 Hz, aromatic), 134.87 (d, J = 9 Hz, aromatic), 134.7 (d, J = 10 Hz, aromatic), 130.5 (d, J = 27 Hz, aromatic), 129.2 (d, J = 2 Hz, aromatic), 128.3 (s), 127.4 (d, J = 10 Hz, aromatic), 92.7 (d, J = 3 Hz, C_5Me_5), 10.8 (s, C_5Me_5). ^{31}P{^{1}H} NMR (202.35 MHz, C_6D_6) δ/ppm: 21.1 (s). m.p. 143 °C (decomposition). Anal calcd for $C_{27}H_{31}$IrNP: C 54.71, H 5.27, N 2.36. Found: C 54.97, H 5.31, N 2.19.

Preparation of [(Cp*Ir)$_2$(μ-H)$_2$(μ-PPh$_2$Py)][OTf]$_2$ (3). In a 50 mL two-necked flask, **1** (403 mg, 0.680 mmol) and [Cp*Ir(NCMe)$_3$][OTf]$_2$ (510 mg, 0.680 mmol) were placed. When acetone (12 mL) was added, the colour of the reaction mixture turned into black and the mixture was stirred for 30 min. After evaporation of volatiles, the residue was extracted with acetone. After evaporation of acetone, the black powder was washed with ether and dried *in vacuo* to give **3** (759 mg, 0.623 mmol, 92%). **3**: ^{1}H NMR (500.00 MHz, acetone-d_6) δ/ppm: 9.66 (1H, d, J = 6 Hz, aromatic), 8.34–8.29 (1H, m, aromatic), 7.99–7.96 (1H, m, aromatic), 7.66 (10H, m, aromatic), 7.35 (1H, s, aromatic), 1.92 (15H, d, J = 2 Hz, Cp*), 1.77 (15H, s, Cp*), –14.78 (2H, d,

J = 15 Hz, Ir–H–Ir). $^{13}C\{^1H\}$ NMR (125.65 MHz, acetone-d_6) δ/ppm: 160.1 (d, J = 9 Hz, aromatic), 158.2 (d, J = 75 Hz, aromatic), 141.4 (d, J = 5 Hz, aromatic), 135.2 (d, J = 11 Hz, aromatic), 133.6 (d, J = 2 Hz, aromatic), 131.3 (s, aromatic), 131.0 (d, J = 11 Hz, aromatic), 130.4 (d, J = 11 Hz, aromatic), 129.1 (s, aromatic), 128.5 (d, J = 62 Hz, aromatic), 122.3 (q, J = 324 Hz, CF_3), 100.5 (d, J = 3 Hz, C_5Me_5), 96.37 (s, C_5Me_5), 10.96 (s, C_5Me_5), 10.17 (s, C_5Me_5). $^{31}P\{^1H\}$ NMR (202.35 MHz, acetone-d_6) δ/ppm: 45.6 (s). m.p. 110–112 °C. Anal calcd for $C_{39}H_{46}F_6Ir_2NO_6PS_2$: C 38.45, H 3.81, N 1.15. Found: C 38.29, H 3.83, N 1.38.

Anion metathesis of 3. In a 30 mL two-necked flask, **3** (118 mg, 0.0967 mmol) and methanol (6 mL) were placed, then sodium tetraphenylborate (19.9 mg, 0.0581 mmol) was added. A dark brown solid precipitated. The precipitate was washed with methanol to give **3-BPh$_4$** in 40% yield (60.0 mg, 0.0385 mmol). Single crystals suitable for X-ray analysis were obtained by slow diffusion of hexane into an acetone solution of **3-BPh$_4$**. **3-BPh$_4$**: ^1H NMR (500.00 MHz, acetone-d_6) δ/ppm: 9.48 (1H, d, J = 6 Hz, aromatic), 8.18 (1H, m, aromatic), 7.99–7.96 (1H, m, aromatic), 7.67–7.51 (10H, m, aromatic), 7.34–7.31 (16H, m, BPh_4), 6.89 (16H, t, J = 7 Hz, BPh_4), 6.74 (8H, t, J = 7 Hz, BPh_4), 1.82 (15H, d, J = 2 Hz, Cp*), 1.63 (15H, s, Cp*), –14.79 (2H, d, J = 15 Hz, Ir–H–Ir). $^{31}P\{^1H\}$ NMR (202.35 MHz, acetone-d_6) δ/ppm: 45.9 (s). m.p. 163–165 °C. Anal calcd for $C_{85}H_{86}B_2Ir_2NP$: C 65.50, H 5.56, N 0.90. Found: C 65.69, H 5.62, N 0.89.

Preparation of [(Cp*Ir)(μ-H)$_2$(μ-PPh$_2$Py)(RhCp*)][OTf]$_2$ (4). In a 50 mL two-necked flask, **1** (166 mg, 0.280 mmol) and [Cp*Rh(NCMe)$_3$][OTf]$_2$ (185 mg, 0.280 mmol) were placed. When acetone (6 mL) was added, the colour of the reaction mixture turned to dark brown and the mixture was stirred for 30 min. After evaporation of volatiles, the residue was extracted with acetone. After evaporation of acetone, the black powder was washed with ether and dried *in vacuo* to give **4** (262 mg, 0.232 mmol, 83%). **4**: ^1H NMR (500.00 MHz, CD_2Cl_2, 253 K) δ/ppm: 9.43 (1H, m, aromatic), 7.99 (1H, m, aromatic), 7.89 (1H, m, aromatic), 7.52 (7H, m, aromatic), 7.23 (4H, m, aromatic), 1.87 (15H, d, J = 2 Hz, Cp*), 1.38 (15H, s, Cp*), –15.30 (2H, t, J = 20 Hz, Ir–*H*–Rh). $^{13}C\{^1H\}$ NMR (125.65 MHz, CD_2Cl_2, 233 K) δ/ppm: 158.0 (d, J = 11 Hz, aromatic), 138.8 (s, aromatic), 133.4 (d, J = 3 Hz, aromatic), 132.3 (s, aromatic), 131.5 (d, J = 10 Hz, aromatic), 130.1 (s, aromatic), 129.2 (d, J = 11 Hz, aromatic), 128.6 (s, aromatic), 126.6 (s, aromatic), 120.5 (q, J = 320 Hz, CF_3), 100.5 (d, J = 6 Hz, C_5Me_5), 96.9 (s, C_5Me_5), 10.2 (s, C_5Me_5), 9.7 (s, C_5Me_5). $^{31}P\{^1H\}$ NMR (202.35 MHz, CD_2Cl_2, 253 K) δ/ppm: 26.1 (s). m.p. 90–92 °C. Anal calcd for $C_{39}H_{46}F_6IrNO_6PRhS_2$: C 41.49, H 4.11, N 1.24. Found: C 41.04, H 4.08, N 1.39.

Preparation of [(Cp*Ir)(μ-H)$_2$(μ-PPh$_2$Py)(RuCp*)][OTf] (5). In a 10 mL Schlenk tube, **1** (26.3 mg, 0.0444 mmol) and [Cp*Ru(NCMe)$_3$][OTf] (21.8 mg, 0.0428 mmol) were placed. When acetone (1 mL) was added, the colour of the reaction mixture turned to green and the mixture was stirred for 30 min. After the evaporation of volatiles, the residue was extracted with acetone. After the evaporation of acetone, the green powder was washed with hexane and dried *in vacuo* to give **5** as a green powder (39.2 mg, 0.0401 mmol, 90%). **5**: ^1H NMR (500.00 MHz, acetone-d_6) δ/ppm: 9.87 (1H, d, J = 5 Hz, aromatic), 7.83 (1H, m, aromatic), 7.63 (1H, m, aromatic), 7.46–7.40 (8H, m, aromatic), 7.10–7.06 (3H, m, aromatic), 1.91 (15H, s, Cp*), 1.32 (15H, s, Cp*), –16.13 (2H, d, J = 20 Hz, Ir–H–Ru). $^{13}C\{^1H\}$ NMR (125.65 MHz, acetone-d_6) δ/ppm: 157.6 (d, J = 11 Hz, aromatic), 136.4 (d, J = 5 Hz, aromatic), 133.9 (d, J = 11 Hz, aromatic), 133.0 (d, J = 58 Hz, aromatic), 131.4 (d, J = 2 Hz, aromatic), 129.0 (d, J = 11 Hz, aromatic), 128.6 (d, J = 12 Hz, aromatic), 121.5 (q, J = 318 Hz, CF_3), 98.2 (s, C_5Me_5), 96.4 (d, J = 2 Hz, C_5Me_5), 10.9 (s, C_5Me_5), 10.5 (s, C_5Me_5). $^{31}P\{^1H\}$ NMR (202.35 MHz, acetone-d_6) δ/ppm: 11.5 (s). m.p. 109–110 °C.

Reaction of ethyne with 3. To an acetone solution (4 mL) of **3** (41.0 mg, 0.0337 mmol) in a 10 mL Schlenk tube, ethyne (1 atm.) was introduced by gas balloon. Stirring for 15 min at room temperature, the dark brown solution turned into a light green solution with a small amount of precipitate. Then the solvent was removed *in vacuo*. The residue was extracted with dichloromethane and washed with hexane to give the orange powder **6** (35.1 mg, 0.0282 mmol, 84%). **6**: ^1H NMR (500.00 MHz, CD_3OD) δ/ppm: 8.68 (1H, d, J = 6 Hz, aromatic), 8.08 (1H, m, aromatic), 7.78 (6H, m, aromatic), 7.66 (2H, m, aromatic), 7.60 (1H, m, aromatic), 7.54 (1H, m, aromatic), 7.35 (1H, ddd, J = 12 Hz, 8 Hz, 2 Hz, Ir–C*H*=CH_2), 7.30 (2H, aromatic), 4.69 (1H, dd, J = 8, 2 Hz, C=C*H*H), 2.81 (1H, ddd, J = 14 Hz, 12 Hz, 2 Hz, C=CH*H*), 1.85 (15H, d, J = 2 Hz, Cp*), 1.79 (15H, s, Cp*), –17.41 (1H, d, J = 31 Hz, Ir–H–Ir). $^{13}C\{^1H\}$ NMR (125.65 MHz, acetone-d_6) δ/ppm: 160.6 (d, J = 85 Hz, aromatic), 160.0 (d, J = 10 Hz, aromatic), 140.4 (d, J = 5 Hz, aromatic), 136.3 (d, J = 11 Hz, aromatic), 134.7 (s, aromatic), 134.3 (s, aromatic), 134.2 (s, aromatic), 134.2 (s, aromatic), 131.4 (d, J = 11 Hz, aromatic), 131.2 (d, J = 10 Hz, aromatic), 130.2 (s, aromatic), 128.0 (d, J = 55 Hz, aromatic), 127.0 (d, J = 67 Hz, aromatic), 121.8 (d, J = 312 Hz, CF_3), 119.5 (s, Ir–*C*H=), 103.5 (d, J = 2 Hz, C_5Me_5), 97.5 (s, C_5Me_5), 54.2 (s, CH=CH_2), 9.9 (s, C_5Me_5), 9.3 (s, C_5Me_5). $^{31}P\{^1H\}$ NMR (202.35 MHz, CD_3OD) δ/ppm: 19.7 (s). m.p. 129 °C (decomposition). Anal calcd for $C_{41}H_{48}F_6Ir_2NO_6PS_2$: C 39.57, H 3.89, N 1.13. Found: C 39.60, H 3.92, N 1.18.

Reaction of methyl propiolate with 3. To an acetone (3 mL) solution of **3** (160 mg, 0.132 mmol) in a 30 mL two-necked flask, methyl propiolate (34.3 mg, 0.48 mmol) was added. Stirring for 15 min at room temperature, the dark brown solution turned into a light orange solution. Then the solvent was removed *in vacuo* and followed by washing with ether to give the pale orange powder **7** (119 mg, 0.914 mmol, 69%). **7**: ^1H NMR (500.00 MHz, acetone-d_6) δ/ppm: 8.86 (1H, d, J = 5 Hz, aromatic), 8.26–8.20 (1H, m, aromatic), 8.00–7.95 (1H, m, aromatic), 7.82 (10H, m, aromatic), 7.69 (1H, s, aromatic), 4.84 (d, 1H, J = 3 Hz, C=CH*H*), 3.87 (3H, s, Me), 2.42 (1H, dd, J = 16 Hz, 3 Hz, C=C*H*H), 1.94 (15H, d, J = 2 Hz, Cp*), 1.87 (15H, s, Cp*), –17.31 (1H, d, J = 31 Hz, Ir–H–Ir). $^{13}C\{^1H\}$ NMR (125.65 MHz, acetone-d_6) δ/ppm: 174.0 (s, C=O), 159.4 (d, J = 10 Hz, aromatic), 159.0 (d, J = 87 Hz, aromatic), 140.7 (d, J = 5 Hz, aromatic), 135.6 (d, J = 10 Hz, aromatic), 135.0 (d, J = 12 Hz, aromatic), 134.7 (d, J = 3 Hz, aromatic), 134.6 (d, J = 2 Hz, aromatic), 134.4 (d, J = 9 Hz, aromatic), 131.2 (d, J = 11 Hz, aromatic), 130.9 (d, J = 62 Hz, aromatic), 130.1 (s), 127.3 (d, J = 54 Hz, aromatic), 126.4 (d, J = 66 Hz, aromatic), 122.3 (q, J = 320 Hz, CF_3), 120.4 (s, Ir–*C*H=, 99.0 (s, C_5Me_5), 52.9 (s, CO_2Me), 46.2 (s, C=CH_2), 9.5 (d, J = 4 Hz, C_5Me_5), 8.3 (s, C_5Me_5). $^{31}P\{^1H\}$ NMR (202.35 MHz,

acetone-d_6) δ/ppm: 20.7 (s). m.p. 104 °C (decomposition). Anal calcd for $C_{43}H_{50}F_6Ir_2NO_8PS_2$: C 39.65, H 3.87, N 1.08. Found: C 39.25, H 3.96, N 1.03.

Reaction of trimethylsilylacetylene with 3. To an acetone (2 mL) solution of **3** (99.5 mg, 0.0817 mmol) in a 10 mL Schlenk tube, trimethylsilylacetylene (44.5 mg, 0.453 mmol) was added. Stirring for 15 min at room temperature, the dark brown solution turned into an orange solution. The solvent was removed *in vacuo*. The residue was washed with hexane and extracted with acetone to give the orange powder **8** (102 mg, 0.0775 mmol, 95%). **8**: ^{1}H NMR (500.00 MHz, acetone-d_6) δ/ppm: 8.88 (1H, d, J = 6 Hz, aromatic), 8.35 (1H, d, J = 17 Hz, Ir–C*H*=C), 8.33–8.31 (1H, m, aromatic), 7.80–7.60 (10H, m, aromatic), 7.30 (2H, m, aromatic), 5.29 (1H, d, J = 17 Hz, CH=C*H*–SiMe$_3$) 1.93 (15H, d, J = 2 Hz, Cp*), 1.88 (15H, s, Cp*), 0.28 (9H, s, Si*Me$_3$*), –17.11 (d, J = 23 Hz, 1H, Ir–H–Ir). ^{13}C{^{1}H} NMR (125.65 MHz, acetone-d_6) δ/ppm: 161.0 (d, J = 9 Hz, aromatic), 155.8 (d, J = 71 Hz, aromatic), 145.9 (d, J = 4 Hz, Ir–*C*H=), 142.0 (d, J = 4 Hz, aromatic), 136.1 (d, J = 12 Hz, aromatic), 135.3 (d, J = 10 Hz, aromatic), 134.3 (d, J = 11 Hz, aromatic), 134.0 (d, J = 2 Hz, aromatic), 133.8 (d, J = 11 Hz, aromatic), 133.3 (d, J = 3 Hz, aromatic), 130.8 (d, J = 11 Hz, aromatic), 130.5 (d, J = 12 Hz, aromatic), 130.3 (d, J = 31 Hz, aromatic), 129.0 (d, J = 64 Hz, aromatic) 122.4 (q, J = 322 Hz, *C*F$_3$), 100.5 (d, J = 2 Hz, *C*$_5$Me$_5$), 99.8 (d, J = 4 Hz, CH=*C*HSiMe$_3$), 98.8 (s, *C*$_5$Me$_5$), 10.8 (s, C$_5$*Me$_5$*), 10.2 (s, C$_5$*Me$_5$*), 1.4 (s, Si*Me$_3$*). ^{31}P{^{1}H} NMR (202.35 MHz, acetone-d_6) δ/ppm: 30.3 (s).

Anion metathesis of 8. In a 30 mL two-necked flask, **8** (102 mg, 0.0775 mmol) was placed. After the addition of methanol, NaBPh$_4$ (46.8 mg, 0.137 mmol) was added to the solution. The precipitate of **8-BPh$_4$** was collected and dried *in vacuo*. Yield 103.4 mg (0.0624 mmol, 81%). **8-BPh$_4$**: ^{1}H NMR (500.00 MHz, acetone-d_6) δ/ppm: 8.75 (d, J = 6 Hz, 1H, aromatic), 8.30 (d, J = 17 Hz, 1H, Ir–C*H*=C), 7.96 (1H, m, aromatic), 7.71–7.58 (m, 10H, aromatic), 7.33 (16H, br, B*Ph$_4$*), 7.23 (m, 2H, aromatic), 6.90 (16H, t, J = 7 Hz, B*Ph$_4$*), 6.76 (8H, t, J = 7 Hz, B*Ph$_4$*) 5.23 (d, J = 17 Hz, CH=C*H*–SiMe$_3$), 1.86 (d, J = 2 Hz, 15H, Cp*), 1.77 (s, 15H, Cp*) 0.27 (s, 9H, SiMe$_3$), –17.19 (d, J = 22 Hz, 1H, Ir–H–Ir). ^{31}P{^{1}H} NMR (109.24 MHz, acetone-d_6) δ/ppm: 29.7 (s). m.p. 168 °C. Anal calcd for $C_{90}H_{96}B_2Ir_2NPSi$: C 65.24, H 5.84, N 0.85. Found: C 65.12, H 5.69, N 0.89.

Reaction of phenylacetylene with 3. To an acetone solution of **3** (191 mg, 0.157 mmol) in a two-necked flask, phenylacetylene (81.2 mg, 0.795 mmol) was added. Stirring for 15 min at room temperature, the dark brown solution turned into a light orange solution. The solvent was removed *in vacuo*. Yields of each isomer were determined by ^{31}P{^{1}H} NMR using an internal standard (**9**: 34%, **10**: 43%). Anal calcd for isomeric mixture of $C_{47}H_{52}F_6Ir_2NO_6PS_2$: C 42.75, H 3.97, N 1.06. Found: C 42.51, H 4.03, N 1.11. Column chromatography on silica gel (eluent: 5% methanol in dichloromethane) gave pure **9** in 16% yield (32.9 mg) as an orange solid. **9**: ^{1}H NMR (500.00 MHz, acetone-d_6) δ/ppm: 9.00 (1H, d, J = 5 Hz, py), 8.27 (1H, t, J = 8 Hz, py), 7.96–7.21 (5H, m, aromatic), 4.86 (1H, d, J = 3 Hz, C=C*H*H), 2.65 (1H, dd, J = 16, 3 Hz, C=CH*H*), 1.69 (15H, d, J = 2 Hz, Cp*), 1.54 (15H, s, Cp*), –17.04 (1H, d, J = 28 Hz, Ir–H–Ir). ^{13}C{^{1}H} NMR (125.65 MHz, acetone-d_6) δ/ppm: 159.8 (d, J = 87, aromatic), 159.6 (d, J = 10 Hz, aromatic), 149.2 (s, aromatic), 146.6 (s, Ir–*C*(Ph)=CH$_2$), 140.5 (d, J = 5 Hz, aromatic), 135.7 (d, J = 10 Hz, aromatic), 135.3 (d, J = 12 Hz, aromatic), 134.6 (d, J = 3 Hz, aromatic), 134.6 (d, J = 3 Hz, aromatic), 134.5 (d, J = 10 Hz, aromatic), 132.4 (s, aromatic), 131.3 (d, J = 11 Hz, aromatic), 130.8 (t, J = 6 Hz, aromatic), 130.3 (s, aromatic), 130.0 (s, aromatic), 128.7 (d, J = 17 Hz, aromatic), 128.4 (s, aromatic), 127.0 (d, J = 65 Hz, aromatic), 122.4 (d, J = 322 Hz, CF$_3$), 104.7 (s, *C*$_5$Me$_5$), 99.2 (s, *C*$_5$Me$_5$), 45.6 (s, C=*C*H$_2$), 10.0 (s, C$_5$*Me$_5$*), 9.6 (s, C$_5$*Me$_5$*). ^{31}P{^{1}H} NMR (202.35 MHz, acetone-d_6) δ/ppm: 21.4 (s).

10 was obtained as a mixture with an unidentified compound. **10**: ^{1}H NMR (500.00 MHz, acetone-d_6) δ/ppm: 8.85 (1H, d, J = 6 Hz, py), 8.37 (1H, t, J = 8 Hz, aromatic), 8.19 (1H, d, J = 14 Hz, Ir–C*H*=CH), 8.01–7.40 (17H, m, aromatic), 6.09 (1H, d, J = 14 Hz, CH=C*H*–Ph), 1.99 (15H, d, J = 2 Hz, Cp*), 1.60 (15H, s, Cp*), –17.21 (1H, d, J = 22 Hz, Ir–H–Ir). ^{13}C{^{1}H} NMR (125.65 MHz, acetone-d_6) δ/ppm: 160.1 (d, J = 8 Hz, aromatic), 156.6 (d, J = 72 Hz, aromatic), 142.1 (d, J = 5 Hz, aromatic), 140.9 (d, J = 4 Hz, Ir–*C*H=CH), 138.6–128.4 (aromatic), 106.5 (d, J = 3 Hz, CH=*C*H–Ph), 100.1 (d, J = 2 Hz, *C*$_5$Me$_5$), 98.4 (s, *C*$_5$Me$_5$), 10.1 (s, C$_5$*Me$_5$*), 9.2 (s, C$_5$*Me$_5$*). ^{31}P{^{1}H} NMR (202.35 MHz, acetone-d_6) δ/ppm: 30.0 (s).

Anion metathesis of 9. **9-BPh$_4$** was obtained by the reaction of **9** (32.9 mg, 0.0253 mmol) with sodium tetraphenylborate (19.9 mg, 0.0581 mmol) in methanol (2 mL). The resulting yellow powder was washed with methanol to give **9-BPh$_4$** in 78% yield. Single crystals suitable for X-ray analysis were obtained by slow diffusion of hexane into acetone solution of **9-BPh$_4$**. **9-BPh$_4$**: ^{1}H NMR (500.00 MHz, acetone-d_6) δ/ppm: 8.85 (1H, d, J = 6 Hz, py), 7.95 (1H, t, J = 9 Hz, py), 7.87–7.77 (5H, m, aromatic), 7.76 (1H, t, J = 7 Hz, aromatic), 7.63 (2H, m, aromatic), 7.51–7.43 (5H, m, aromatic), 7.32 (16H, br, B*Ph$_4$*), 7.26–7.15 (3H, m, aromatic), 6.89 (16H, t, J = 7 Hz, B*Ph$_4$*), 6.75 (8H, t, J = 7 Hz, B*Ph$_4$*), 4.74 (1H, d, J = 2 Hz, C=C*H*H), 2.57 (1H, dd, J = 16, 2 Hz, C=CH*H*), 1.61 (15H, d, J = 2 Hz, Cp*), 1.46 (15H, s, Cp*), –17.14 (1H, d, J = 28 Hz, Ir–H–Ir). ^{31}P{^{1}H} NMR (202.35 MHz, acetone-d_6) δ/ppm: 21.3 (s). m.p. 195 °C (decomposition). Anal calcd for $C_{93}H_{92}B_2Ir_2NP{\cdot}C_3H_6O$: C 67.08, H 5.75, N 0.81. Found: C 66.80, H 5.75, N 0.80.

Reaction of ethyne with 4. To an acetone solution of **4** (141 mg, 0.220 mmol) in a two-necked flask, ethyne (1 atm.) was introduced by gas balloon. Stirring for 15 min at room temperature, the dark brown solution turned into a red solution. The solvent was removed *in vacuo*. The residue was column chromatographed on silica gel (eluent: 10% methanol in dichloromethane) to give **11a** as a red powder (223 mg, 0.192 mmol, 87%). **11a**: ^{1}H NMR (500.00 MHz, acetone-d_6) δ/ppm: 8.70 (1H, d, J = 6 Hz, py), 8.20 (1H, t, J = 7 Hz, py), 7.91–7.65 (10H, m, aromatic), 7.47 (1H, m, Rh–C*H*=CH$_2$), 7.37 (2H, m, aromatic), 4.28 (1H, dd, J = 7 Hz, 2 Hz, CH=C*H*H), 3.10 (1H, ddd, J = 13 Hz, 12 Hz, 2 Hz, CH=CH*H*), 1.93 (15H, d, J = 2 Hz, Cp*), 1.79 (15H, s, Cp*), –17.42 (dd, J = 31 Hz, 20 Hz, Ir–H–Rh). ^{13}C{^{1}H} NMR (125.65 MHz, acetone-d_6) δ/ppm: 159.2 (d, J = 88 Hz, aromatic), 158.2 (d, J = 11 Hz, aromatic), 142.3 (d, J = 28 Hz, Rh–*C*H), 140.4 (d, J = 5 Hz, aromatic), 135.8 (d, J = 10 Hz, aromatic), 134.1 (s, aromatic), 134.0 (s, aromatic), 133.8 (d, J = 13 Hz, aromatic), 131.1 (d, J = 11 Hz, aromatic),

130.8 (d, J = 11 Hz, aromatic), 129.3 (s, aromatic), 127.5 (d, J = 54 Hz, aromatic), 127.2 (d, J = 70 Hz, aromatic), 126.2 (s), 122.3 (q, J = 323 Hz, CF_3), 103.9 (s, C_5Me_5), 103.0 (s, C_5Me_5), 55.7 (s, CH=CH_2), 10.2 (s, C_5Me_5), 9.4 (s, C_5Me_5). $^{31}P\{^1H\}$ NMR (202.35 MHz, acetone-d_6) δ/ppm: 16.7 (s). m.p. 70 °C (decomposition).

Reaction of methyl propiolate with 4. To an acetone (2 mL) solution of **4** (90.1 mg, 0.0798 mmol) in a two-necked flask, methyl propiolate (14.6 mg, 0.173 mmol) was added. Stirring for 15 min at room temperature, the dark brown solution turned into a red solution. The solvent was removed *in vacuo*. The residue was extracted with a minimum volume of acetone, and evaporation of acetone gave **12a** as a red powder (82.4 mg, 0.0679 mmol, 85%). **12a**: ^1H NMR (500.00 MHz, acetone-d_6) δ/ppm: 8.90 (1H, d, J = 5 Hz, aromatic), 8.23 (1H, m, aromatic), 7.93–7.70 (9H, m, aromatic), 7.45 (1H, m, aromatic), 7.29 (m, 2H, aromatic), 4.15 (br, 1H, C=CHH), 3.87 (3H, s, CO_2Me), 2.64 (dd, J = 15 Hz, 2 Hz, C=CHH), 1.95 (15H, d, J = 2 Hz, Cp*), 1.65 (15H, s, Cp*), −16.95 (dd, J = 29 Hz, 20 Hz, Ir–H–Rh). $^{13}C\{^1H\}$ NMR (125.65 MHz, acetone-d_6) δ/ppm: 172.9 (s, CO_2Me), 158.1 (d, J = 88 Hz, aromatic), 157.6 (d, J = 12 Hz, aromatic), 140.8 (d, J = 12 Hz, aromatic), 137.9 (d, J = 26 Hz, Rh–C(CO_2Me)=), 135.4 (d, J = 10 Hz, aromatic), 135.0 (d, J = 13 Hz, aromatic), 134.6 (s, aromatic), 134.4 (d, J = 9 Hz, aromatic), 131.3 (d, J = 11 Hz, aromatic), 130.8 (d, J = 10 Hz, aromatic), 129.4 (s, aromatic), 127.2 (d, J = 51 Hz, aromatic), 127.2 (d, J = 66 Hz, aromatic), 122.3 (q, J = 323 Hz, CF_3), 106.6 (s, C_5Me_5), 104.9 (d, J = 6 Hz, C_5Me_5), 52.7 (s, CO_2Me), 46.6 (s, C=CH_2), 9.8 (s, C_5Me_5), 9.6 (s, C_5Me_5). $^{31}P\{^1H\}$ NMR (202.35 MHz, acetone-d_6) δ/ppm: 15.8 (s). m.p. 92 °C (decomposition).

Isomerization of 12a. Heating an acetone solution of **12a** at 50 °C for 5 h resulted in the equilibrium of **12a** and **12b** (0.6 : 0.4). The ratio was determined by NMR. **12b**: ^1H NMR (500.00 MHz, acetone-d_6) δ/ppm: 8.66 (1H, d, J = 5 Hz, aromatic), 8.27 (1H, m, aromatic), 7.96–7.69 (m, aromatic), 7.21 (1H, s, C=CHH), 5.04 (1H, s, C=CHH), 3.32 (3H, s, CO_2Me), 1.91 (15H, d, J = 2 Hz, Cp*), 1.74 (15H, s, Cp*), −17.07 (1H, t, J = 22 Hz, Ir–H–Rh). $^{13}C\{^1H\}$ NMR (125.65 MHz, acetone-d_6) δ/ppm: 171.5 (s, CO_2Me), 160.1 (d, J = 10 Hz, aromatic), 158.5 (d, J = 72 Hz, aromatic), 146.9 (m, Ir–C(CO_2Me)=), 141.0 (d, J = 5 Hz, aromatic), 135.7 (br, aromatic), 134.7 (d, J = 11 Hz, aromatic), 133.5 (d, J = 41 Hz, aromatic), 132.9 (d, J = 11 Hz, aromatic), 131.7 (d, J = 65 Hz, aromatic), 131.3 (d, J = 11 Hz, aromatic), 130.8 (d, J = 10 Hz, aromatic), 129.9 (d, J = 10 Hz, aromatic), 129.5 (s, aromatic), 129.1 (d, J = 52 Hz), 122.3 (q, J = 323 Hz, CF_3), 107.2 (d, J = 7 Hz, C_5Me_5), 100.4 (s, C_5Me_5), 98.7 (s, C=CH_2), 53.7 (s, CO_2Me), 10.5 (s, C_5Me_5), 9.9 (s, C_5Me_5). $^{31}P\{^1H\}$ NMR (202.35 MHz, acetone-d_6) δ/ppm: 18.5 (s).

Reaction of phenylacetylene with 4. To an acetone solution (5 mL) of **4** (275 mg, 0.243 mmol) in a two-necked 30 mL flask, phenylacetylene (115 mg, 1.13 mmol) was added. Stirring for 15 min at room temperature, the dark brown solution turned into a red solution. After evaporation of the solvent, the residue was chromatographed on silica-gel with an ice-bath jacket (eluent: 5% methanol in dichloromethane) to give pure **13a** as a red powder in 72% isolated yield. **13a**: ^1H NMR (500.00 MHz, acetone-d_6) δ/ppm: 8.83 (1H, d, J = 5 Hz, py), 8.22 (1H, t, J = 8 Hz, py), 7.98–7.24 (17H, m, aromatic), 4.15 (1H, d, J = 4 Hz, C=CHH), 2.74 (1H, dd, J = 16 Hz, 4 Hz, C=CHH), 1.69 (15H, d, J = 2 Hz, Cp*), 1.42 (15H, s, Cp*), −16.66 (1H, dd, J = 29 Hz, 20 Hz, Ir–H–Rh). $^{13}C\{^1H\}$ NMR (125.65 MHz, acetone-d_6) δ/ppm: 164.7 (d, J = 23 Hz, Rh–C=C), 159.1 (d, J = 89 Hz, aromatic), 157.7 (d, J = 11 Hz, aromatic), 148.6 (s, aromatic), 140.5 (d, J = 6 Hz, aromatic), 135.4 (d, J = 11 Hz, aromatic), 135.2 (d, J = 13 Hz, aromatic), 134.5 (d, J = 2 Hz, aromatic), 134.4 (s, aromatic), 134.3 (s, aromatic), 131.3 (d, J = 11 Hz, aromatic), 130.6 (d, J = 11 Hz, aromatic), 130.0 (s, aromatic), 129.2 (s, aromatic), 128.5 (s, aromatic), 128.4 (d, J = 59 Hz, aromatic), 127.4 (d, J = 65 Hz, aromatic), 122.4 (d, J = 325 Hz, CF_3), 105.7 (s, C_5Me_5), 105.1 (d, J = 6 Hz, C_5Me_5), 45.8 (s, C=CH_2), 10.3 (s, C_5Me_5), 9.6 (s, C_5Me_5). $^{31}P\{^1H\}$ NMR (202.35 MHz, acetone-d_6) δ/ppm: 16.8 (s). m.p. 87 °C (decomposition). Anal calcd for $C_{47}H_{52}F_6IrNO_6PRhS_2$: C 45.85, H 4.26, N 1.14. Found: C 45.67, H 4.37, N 1.01.

Isomerization of 13a. Heating an acetone solution of **13a** at 50 °C for 5 h resulted in the equilibrium of **13a** and **13b** (0.1 : 0.9). The ratio was determined by NMR. **13b**: ^1H NMR (500.00 MHz, acetone-d_6) δ/ppm: 8.77 (1H, d, J = 6 Hz, py), 7.84–7.17 (18H, m, aromatic), 6.61 (1H, s, C=CHH), 5.01 (1H, s, C=CHH), 1.91 (15H, d, J = 2 Hz, Cp*), 1.72 (15H, s, Cp*), −17.64 (1H, t, J = 23 Hz, Ir–H–Rh). $^{13}C\{^1H\}$ NMR (125.65 MHz, acetone-d_6) δ/ppm: 171.1 (brs, Ir–C=C), 159.9 (d, J = 12 Hz, aromatic), 156.6 (d, J = 75 Hz, aromatic), 146.5 (d, J = 3 Hz, aromatic), 139.7 (d, J = 5 Hz, aromatic), 135.6 (br s, aromatic), 134.0 (d, J = 10 Hz, aromatic), 133.5 (d, J = 2 Hz, aromatic), 133.1 (d, J = 2 Hz, aromatic), 132.2 (d, J = 11 Hz, aromatic), 132.2 (d, J = 65 Hz, aromatic), 130.6 (d, J = 21 Hz, aromatic), 130.1 (d, J = 11 Hz, aromatic), 129.9 (s, aromatic), 129.0 (d, J = 52 Hz, aromatic), 128.9 (s, aromatic), 122.34 (d, J = 322 Hz, CF_3), 106.3 (d, J = 7 Hz, C_5Me_5), 100.5 (s, C_5Me_5), 86.0 (d, J = 5 Hz, C=CH_2), 10.5 (s, C_5Me_5), 9.7 (s, C_5Me_5). $^{31}P\{^1H\}$ NMR (202.35 MHz, acetone-d_6) δ/ppm: 15.3 (s).

Anion metathesis of 13b. **13b-BPh_4** was obtained by the reaction of 1 : 9 mixture of **13a** and **13b** (123 mg, 0.100 mmol) with sodium tetraphenylborate (76.0 mg, 0.222 mmol) in methanol (8 mL). The resulting red powder was washed with methanol to give **13a-BPh_4** and **13b-BPh_4** in 87% yield (138 mg. 0.0874 mmol). Single crystals of **13b-BPh_4** suitable for X-ray analysis were obtained by slow diffusion of hexane into acetone solution of the mixture of **13a-BPh_4** and **13b-BPh_4**. **13b-BPh_4**: ^1H NMR (500.00 MHz, acetone-d_6) δ/ppm: 8.74 (1H, d, J = 5 Hz, py), 7.83–7.37 (16H, m, aromatic), 7.33 (16H, br, BPh_4), 7.23 (2H, m, aromatic), 6.91 (16H, t, J = 7 Hz, BPh_4), 6.77 (8H, t, J = 7 Hz, BPh_4), 6.68 (1H, s, C=CHH), 5.01 (1H, s, C=CHH), 1.92 (15H, d, J = 2 Hz, Cp*), 1.73 (15H, s, Cp*), −17.58 (t, J = 22 Hz, Ir–H–Rh). $^{31}P\{^1H\}$ NMR (202.35 MHz, acetone-d_6) δ/ppm: 15.8 (s).

Reaction of methyl propiolate with 5. In a 30 mL two-necked flask, **1** (160 mg, 0.270 mmol) and [Cp*Ru(NCMe)$_3$][OTf] (137 mg, 0.270 mmol) were placed. Acetone (4 mL) was added to the flask, then the colour of the reaction mixture turned green. After stirring for 10 min, methyl propiolate (71.7 mg, 0.853 mmol) was added, and the reaction mixture was stirred for 15 min. After evaporation of solvent, the residue was chromatographed on silica-gel (eluent: 5% methanol in dichloromethane) to give **14b** as a red powder in 64% yield (183 mg, 0.172 mmol). **14b**: ^1H NMR (500.00 MHz, acetone-d_6) δ/ppm: 8.30 (1H, d, J = 6 Hz, py), 7.95–7.91 (1H, m,

aromatic), 7.70–7.13 (12H, m, aromatic), 5.99 (1H, s, C=CH*H*), 3.85 (1H, s, C=C*H*H), 3.19 (3H, s, CO_2*Me*), 1.75 (15H, d, J = 2 Hz, Cp*), 1.45 (15H, s, Cp*), –19.94 (1H, d, J = 28 Hz, Ir–H–Ru). $^{13}C\{^1H\}$ NMR (125.65 MHz, acetone-d_6) δ/ppm: 174.9 (s, *C*O_2Me), 161.4 (d, J = 77 Hz, aromatic), 159.5 (d, J = 11 Hz, aromatic), 137.2 (d, J = 5 Hz, aromatic), 136.1 (d, J = 10 Hz, aromatic), 135.7 (d, J = 9 Hz, aromatic), 134.7 (s, aromatic), 133.9 (d, J = 65 Hz, aromatic), 132.6 (d, J = 50 Hz, aromatic), 132.4 (d, J = 3 Hz, aromatic), 132.1 (d, J = 2 Hz, aromatic), 131.0 (d, J = 11 Hz, aromatic), 129.9 (d, J = 10 Hz, aromatic), 129.2 (d, J = 10 Hz, aromatic), 122.5 (q, J = 322 Hz, *C*F_3), 115.6 (d, J = 6 Hz, Ir–*C*=CH_2), 97.1 (d, J = 3 Hz, *C*$_5$Me$_5$), 88.7 (s, *C*$_5$Me$_5$), 77.5 (s, Ir–C=*C*H_2), 52.3 (s, CO_2*Me*), 10.2 (s, C$_5$*Me*$_5$), 9.8 (s, C$_5$*Me*$_5$). $^{31}P\{^1H\}$ NMR (202.35 MHz, acetone-d_6) δ/ppm: 12.9 (s). m.p. 120 °C (decomposition). Anal calcd for $C_{45}H_{56}F_3IrNO_6PRuS$: C 47.49, H 4.74, N 1.32. Found: C 47.79, H 4.95, N 1.19.

Table 3 Crystal data and structure refinement parameters for **3-BPh$_4$**, **8-BPh$_4$**, **9-BPh$_4$**, **13b-BPh$_4$**, **14b** and **15b**

	3-BPh$_4$	**8**-BPh$_4$	**9**-BPh$_4$·(C_3H_6O)	**13b**-BPh$_4$·(C_3H_6O)	**14b**·(C_3H_6O)	**15b**
Description of the crystals						
Colour, habit	Red, block	Orange, block	Orange, block	Red, platelet	Orange, block	Orange, prism
Max. crystal dimensions/mm	0.25 × 0.20 × 0.15	0.48 × 0.48 × 0.28	0.30 × 0.20 × 0.10	0.17 × 0.12 × 0.06	0.45 × 0.35 × 0.25	0.33 × 0.25 × 0.15
Crystal system	Monoclinic	Orthorhombic	Triclinic	Triclinic	Monoclinic	Triclinic
Space group	$P2_1/a$ (#14)	$Pbca$ (#61)	$P\bar{1}$ (#2)	$P\bar{1}$ (#2)	$P21/c$ (#14)	$P\bar{1}$ (#2)
a/Å	18.8004(4)	18.3200 (3)	14.2956(3)	13.9146(4)	15.5336(3)	11.8483(3)
b/Å	18.6689(4)	18.9064(3)	23.5089(4)	15.6332(4)	35.6004(6)	11.9702(3)
c/Å	20.2230(4)	45.7263(8)	26.6374(6)	18.0394(6)	15.9795(3)	15.2344(3)
α/°	90	90	111.4064(8)	90.8843(10)	90	85.5897(7)
β/°	92.8600(8)	90	103.1060(8)	96.7389(10)	90.9470(7)	79.8619(7)
γ/°	90	90	99.0113(7)	90.0164(7)	90	81.6182(8)
V/Å^3	7089.1(3)	15838.0(5)	7829.5(3)	3896.51(19)	8835.5(3)	2101.28(8)
Z	4	8	4	2	8	2
Formula	$C_{85}H_{86}B_2Ir_2NP$	$C_{90}H_{96}B_2Ir_2NSiP$	$C_{96}H_{98}B_2Ir_2NPO$	$C_{96}H_{98}B_2IrRhNPO$	$C_{45}H_{56}IrRuNPO_6F_3S$	$C_{46}H_{52}IrRuNPO_3F_3S$
FW	1558.65	1656.87	1718.87	1629.56	1120.26	1080.24
D_{calcd}/g cm^{-3}	1.460	1.390	1.458	1.389	1.684	1.707
Data Collection						
Radiation, λ/Å	MoKα, λ = 0.71075	MoKα, λ = 0.71075	MoKα, λ = 0.71075	MoKα, λ = 0.71075	MoKα, λ = 0.71075	MoKα, λ = 0.71075
T/K	173(1)	173(1)	173(1)	173(1)	173(1)	173(1)
No. of data images	110	440	110	73	110	44
ω Oscillation range/° (χ = 45.0)	130.0–190.0 (ϕ = 90.0)	130.0–190.0 (ϕ = 30.0)	130.0–190.0 (ϕ = 0.0)	130.0–190.0 (ϕ = 30.0)	130.0–190.0 (ϕ = 120.0)	130.0–190.0 (ϕ = 0.0)
Exposure rate/s °$^{-1}$	240	240	300	300	240	240
ω Oscillation range/° (χ = 45.0)	0.0–160.0 (ϕ = 270.0)	0.0–160.0 (ϕ = 180.0)	0.0–160.0 (ϕ = 210.0)	0.0–159.0 (ϕ = 180.0)	0.0–160.0 (ϕ = 270.0)	0.0–160.0 (ϕ = 180.0)
Exposure rate/s °$^{-1}$	240	240	300	300	240	240
Detector position/mm	127.40	127.40	127.40	127.40	127.40	127.40
Pixel size/mm	0.100	0.100	0.100	0.100	0.100	0.100
$2\theta_{max}$/°	54.96	54.98	54.96	54.94	54.96	54.94
No. of reflections measured	Total: 69 523, unique: 16 228 (R_{int} = 0.069)	Total: 139 956, unique: 18 126 (R_{int} = 0.081)	Total: 76 156, unique: 34 429 (R_{int} = 0.059)	Total: 38 442, unique: 17 671 (R_{int} = 0.097)	Total: 86 656, unique: 20 209 (R_{int} = 0.069)	Total: 20 812, unique: 9541 (R_{int} = 0.040)
Structure determination						
No. of observations	10 149 ($I > 2.00\sigma(I)$)	9174 ($I > 2.00\sigma(I)$) 10 067 ($I > 1.50\sigma(I)$)	21 876 ($I > 2.00\sigma(I)$)	9134 ($I > 2.00\sigma(I)$) 10 358 ($I > 1.50\sigma(I)$)	14 026 ($I > 2.00\sigma(I)$)	9541 ($I > 2.00\sigma(I)$) 7827 ($I > 3.00\sigma(I)$)
No. of variables	912	969	2049	1025	1173	569
Reflection/parameter ratio	11.20	10.39	10.76	10.11	12.02	13.76
Absorption correction	Multi-scan	Numerical	Multi-scan	Multi-scan	Multi-scan	Multi-scan
Transmission factor	0.268–0.563	0.187–0.381	0.211–0.706	0.547–0.887	0.153–0.416	0.316–0.576
R^a	0.0292	0.0452	0.0407	0.0516	0.0406	0.0351
$R_w{}^a$	0.0404[b]	0.0614[c]	0.0507[d]	0.0609[e]	0.0526[f]	0.0461[g]
Goodness of fit	1.013	1.080	1.010	0.984	1.000	1.012
CCDC number	701920	701921	701922	707683	701923	701924

[a] $R = \sum\|F_o|-|F_c\|/\Sigma|F_o|$, $R_w = [\sum w(|F_o|-|F_c|)^2/\sum wF_o^2]^{1/2}$ ($I > 2.00\sigma(I)$). [b] $w = 1/[0.0008F_o^2 + 0.2200\sigma(F_o^2)]$. [c] $w = 1/[1.0000\sigma(F_o^2)]$. [d] $w = 1/[0.0006F_o^2 + 1.0000\sigma(F_o^2)]$. [e] $w = 1/[0.0008F_o^2 + 1.0000\sigma(F_o^2)]$. [f] $w = 1/[0.0003F_o^2 + 1.0000\sigma(F_o^2)]$. [g] $w = 1/[0.0007F_o^2 + 1.0000\sigma(F_o^2)]$.

Reaction of phenylacetylene with 5. In a 10 mL Schlenk tube, **1** (62.2 mg, 0.105 mmol) and [Cp*Ru(NCMe)$_3$][OTf] (53.4 mg, 0.105 mmol) were placed. Acetone (4 mL) was added to the flask, then the colour of reaction mixture turned green. After stirring for 10 min, phenylacetylene (22.6 mg, 0.221 mmol) was added, and the reaction mixture was stirred for 15 min. After evaporation of the solvent, the residue was chromatographed on silica-gel (eluent: 5% methanol in dichloromethane) to give **15b** as a red powder in 96% yield (109 mg, 0.101 mmol). **15b**: ^{1}H NMR (500.00 MHz, acetone-d$_6$) δ/ppm: 8.40 (1H, d, J = 6 Hz, aromatic), 8.03–6.85 (m, aromatic), 5.39 (1H, s, C=C*H*H), 4.18 (1H, s, C=CH*H*), 1.80 (15H, d, J = 2 Hz, Cp*), 1.50 (15H, s, Cp*), −19.83 (1H, d, J = 27 Hz, Ir–H–Ru). ^{13}C{^{1}H} NMR (125.65 MHz, acetone-d$_6$) δ/ppm: 160.0 (d, J = 11 Hz, aromatic), 158.6 (d, J = 78 Hz, aromatic), 150.5 (s, C=C-C_{ipso}), 135.9 (d, J = 5 Hz, aromatic), 134.7 (d, J = 10 Hz, aromatic), 133.9 (d, J = 10 Hz, Ir-*C*(Ph)=C), 132.7 (s, aromatic), 132.6 (s, aromatic), 132.6 (s, aromatic), 132.5 (d, J = 5 Hz, aromatic), 132.3 (s, aromatic), 131.9 (s, aromatic), 130.4 (d, J = 12 Hz, aromatic), 129.9 (d, J = 11 Hz, aromatic), 129.4 (d, J = 10 Hz, aromatic), 128.1 (s, aromatic), 126.6 (s, aromatic), 126.4 (s, aromatic), 122.5 (q, J = 321 Hz, *C*F$_3$), 97.4 (d, J = 3 Hz, C_5Me$_5$), 87.8 (s, C_5Me$_5$), 75.6 (s, C=*C*H$_2$), 10.3 (s, C$_5$*Me*$_5$), 9.7 (s, C$_5$*Me*$_5$). ^{31}P{^{1}H} NMR (202.35 MHz, acetone-d$_6$) δ/ppm: 9.4 (s). m.p. 105 °C (decomposition). Anal calcd for $C_{46}H_{52}F_3IrNO_3PRuS$: C 51.15, H 4.85, N 1.30. Found: C 51.24, H 4.88, N 1.29.

X-Ray crystallographic study of 3-BPh$_4$, 8-BPh$_4$, 9-BPh$_4$, 13b-BPh$_4$, 14b, and 15b. The crystal data and experimental details for **3-BPh$_4$**, **8-BPh$_4$**, **9-BPh$_4$**, **13b-BPh$_4$**, **14b**, and **15b** are summarized in Table 3. Diffraction data were obtained with a Rigaku RAXIS RAPID instrument. Reflection data were corrected for Lorentz and polarization effects. Empirical absorption corrections were applied for **3-BPh$_4$**, **9-BPh$_4$**, **13b-BPh$_4$**, **14b**, and **15b**. Numerical absorption corrections were applied for **8-BPh$_4$**. The structures of **3-BPh$_4$**, **8-BPh$_4$**, **9-BPh$_4$**, **13b-BPh$_4$**, and **14b** were solved by the heavy-atom Patterson method[27,28] and the structure of and **15b** was solved by direct method,[28,29] and refined anisotropically for non-hydrogen atoms by full-matrix least-squares calculations. Atomic scattering factors and anomalous dispersion terms were taken from the literature.[30] The locations of the metal hydrides in **3-BPh$_4$** and **15b** were determined from Fourier difference map. The locations of the metal hydrides in **8-BPh$_4$**, **9-BPh$_4$**, **13b-BPh$_4$**, and **14b** could not be determined. Other hydrogen atoms were located on the idealized positions. In **9-BPh$_4$** and **14b**, there were two independent molecules, which are very similar to each other, in the unit cell, respectively. The calculations were performed using the program system CrystalStructure.[31,32]

Acknowledgements

We thank Dr Mikio Yamasaki of RIGAKU Corporation for his advice on the X-ray study of the complex **8-BPh$_4$** (determination of the lattice parameters and the space group). This work was partially supported by a grant-in-aid for young scientists (B) from the Ministry of Education, Culture, Sports, Science and Technology, Japan.

Notes and references

1 (*a*) L. A. Oro and E. Sola, in *Recent advances in hydride chemistry*, ed. M. Peruzzini and R. Poli, Elsevier, Amsterdam, 2001, ch. 10, pp. 299–327; (*b*) L. M. Venanzi, *Coord. Chem. Rev.*, 1982, **43**, 251; (*c*) H. D. Kaesz and R. B. Saillant, *Chem. Rev.*, 1972, **72**, 231.

2 Recent examples: (*a*) E. B. Walczuk, P. C. J. Kamer and P. W. N. M. van Leeuwen, *Angew. Chem., Int. Ed.*, 2003, **42**, 4665; (*b*) C. A. Sandoval, T. Ohkuma, K. Muñiz and R. Noyori, *J. Am. Chem. Soc.*, 2003, **125**, 13490; (*c*) K. Umezawa-Vizzini and T. R. Lee, *Organometallics*, 2004, **23**, 1448; (*d*) X. Li, T. Vogel, C. D. Incarvito and R. H. Crabtree, *Organometallics*, 2005, **24**, 62; (*e*) H. Wadepohl, U. Kohl, M. Bittner and H. Köppel, *Organometallics*, 2005, **24**, 2097; (*f*) C. S. Weinert, P. E. Fanwick and I. P. Rothwell, *Organometallics*, 2005, **24**, 5759; (*g*) A. R. Sadique, E. A. Gregory, W. W. Brennessel and P. L. Holland, *J. Am. Chem. Soc.*, 2007, **129**, 8112; (*h*) M. Sparta, K. J. Børve and V. R. Jensen, *J. Am. Chem. Soc.*, 2007, **129**, 8487; (*i*) A. Comas-Vives, G. Ujaque and A. Lledós, *Organometallics*, 2007, **26**, 4135; (*j*) L.-C. Liang, P.-S. Chien and P.-Y. Lee, *Organometallics*, 2008, **27**, 3082.

3 (*a*) M. A. Alvarez, M. E. García, V. Riera and M. A. Ruiz, *J. Am. Chem. Soc.*, 1993, **115.**, 3786; (*b*) H. Suzuki, H. Omori, D. H. Lee, Y. Yoshida, M. Fukushima, M. Tanaka and Y. Moro-oka, *Organometallics*, 1994, **13**, 1129; (*c*) D. A. Vicic and W. D. Jones, *Organometallics*, 1999, **18**, 134; (*d*) M. A. Alvarez, M. E. García, V. Riera and M. A. Ruiz, *Organometallics*, 1999, **18**, 634; (*e*) J. R. Torkelson, F. H. Antwi-Nsiah, R. McDonald, M. Cowie, J. G. Pruis, K. J. Jalkanen and R. L. DeKock, *J. Am. Chem. Soc.*, 1999, **121**, 3666; (*f*) T. Shima and H. Suzuki, *Organometallics*, 2000, **19**, 2420; (*g*) D. Ristic-Petrovic, J. R. Tokelson, R. W. Hilts, R. McDonald and M. Cowie, *Organometallics*, 2000, **19**, 4432; (*h*) Y. Yuan, M. V. Jiménez, E. Sola, F. J. Lahoz and L. A. Oro, *J. Am. Chem. Soc.*, 2002, **124**, 752; (*i*) N. Tsukada, T. Mitsuboshi, H. Setoguchi and Y. Inoue, *J. Am. Chem. Soc.*, 2003, **125**, 12102; (*j*) K. Ishiwata, S. Kuwata and T. Ikariya, *Organometallics*, 2006, **25**, 5847; (*k*) T. Kawashima, T. Takao and H. Suzuki, *J. Am. Chem. Soc.*, 2007, **129**, 11006.

4 (*a*) K. Fujita, T. Hamada and R. Yamaguchi, *J. Chem. Soc., Dalton Trans.*, 2000, 1931; (*b*) K. Fujita, H. Nakaguma, F. Hanasaka and R. Yamaguchi, *Organometallics*, 2002, **21**, 3749; (*c*) K. Fujita, H. Nakaguma, T. Hamada and R. Yamaguchi, *J. Am. Chem. Soc.*, 2003, **125**, 12368; (*d*) Y. Takahashi, M. Nonogawa, K. Fujita and R. Yamaguchi, *Dalton Trans.*, 2008, 3546.

5 (*a*) R. R. Burch, A. J. Shusterman, E. L. Muetterties, R. G. Teller and J. M. Williams, *J. Am. Chem. Soc.*, 1983, **105**, 3546; (*b*) F. J. G. Alonso, V. Riera, M. A. Ruiz, A. Tripicchio and M. T. Camellini, *Organometallics*, 1992, **11**, 370; (*c*) G. Hogarth and M. H. Lavender, *J. Chem. Soc., Dalton Trans.*, 1992, 2759; (*d*) M. K. Anwar, G. Hogarth, O. S. Senturk, W. Clegg, S. Doherty and M. R. J. Elsegood, *J. Chem. Soc., Dalton Trans.*, 2001, 341; (*e*) J. A. Cabeza, I. del Rio, F. Grepioni, M. Morento, V. Riera and M. Suárez, *Organometallics*, 2001, **20**, 4190; (*f*) Y. Gao, M. C. Jennings and R. J. Puddephatt, *Dalton Trans.*, 2003, 261; (*g*) G. Banditelli and A. L. Bandini, *Organometallics*, 2006, **25**, 1578; (*h*) M. A. Alvarez, M. E. García, A. Ramos, M. A. Ruiz, M. Lanfranchi and A. Tripicchio, *Organometallics*, 2007, **26**, 5454.

6 Publications on the reactivity of multinuclear complexes without hydrides towards alkynes: (*a*) X. L. R. Fontaine, G. B. Jacobson, B. L. Shaw and M. Thornton-Pett, *J. Chem. Soc., Chem. Commun.*, 1987, 662; (*b*) J. S. Field, R. J. Haines, J. Sundermeyer and S. F. Woollam, *J. Chem. Soc., Chem. Commun.*, 1991, 1382; (*c*) T. Murahashi, T. Otani, T. Okuno and H. Kurosawa, *Angew. Chem., Int. Ed.*, 2000, **39**, 537; (*d*) M. Akita, S. Sugimoto, H. Hirakawa, S. Kato, M. Terada, M. Tanaka and Y. Moro-oka, *Organometallics*, 2001, **20**, 1555; (*e*) R. Ros, A. Tassan, R. Roulet, V. Duprez, S. Detti, G. Laurenczy and K. Schlenk, *J. Chem. Soc., Dalton Trans.*, 2001, 2858; (*f*) T. Murahashi, T. Okuno, T. Nagai and H. Kurosawa, *Organometallics*, 2002, **21**, 3679; (*g*) S. Tanaka, C. Dubs, A. Inagaki and M. Akita, *Organometallics*, 2004, **23**, 317; (*h*) S. Takemoto, T. Kobayashi and H. Matsuzaka, *J. Am. Chem. Soc.*, 2004, **126**, 10802; (*i*) S. Tanaka, C. Dubs, A. Inagaki and M. Akita, *Organometallics*, 2005, **24**, 163; (*j*) M. A. Alvarez, Y. Anaya, M. E. García, M. A. Ruiz and J. Vaissermann, *Organometallics*, 2005, **24**, 2452; (*k*) G. Higashihara, M. Terada, A. Inagaki and M. Akita, *Organometallics*, 2007, **26**, 439.

7 The reactivity of μ-vinyl complexes: (*a*) S. A. R. Knox, *Pure Appl. Chem.*, 1984, **56**, 81; (*b*) S. A. R. Knox, *J. Organomet. Chem.*, 1990, **400**, 255; (*c*) S. A. R. Knox, *J. Cluster Sci.*, 1992, **3**, 385.

8 The insertions of alkynes to mono- or trihydrido-bridged hetero-dinuclear complexes have been reported: (*a*) A. D. Hortron, A. C. Kemball and M. J. Mays, *J. Chem. Soc., Dalton Trans.*, 1988, 2953; (*b*) A. J. M. Caffyn, M. J. Ways and P. R. Raithby, *J. Chem. Soc., Dalton Trans.*, 1992, 515; (*c*) T. Shima and H. Suzuki, *Organometallics*,

2000, **19**, 2420; (*d*) R. D. Adams, B. Captain and L. Zhu, *J. Am. Chem. Soc.*, 2006, **128**, 13672; (*e*) R. D. Adams, B. Captain, E. Trufan and L. Zhu, *J. Am. Chem. Soc.*, 2007, **129**, 7545.

9 Z. Zhang and H. Cheng, *Coord. Chem. Rev.*, 1996, **147**, 1, and references cited therein.

10 During the course of the present study, Govindaswamy *et al.* reported the preparation of **2** by the similar reaction: P. Govindaswamy, P. J. Carroll, Y. A. Mozharivskyj and M. R. Kollipara, *J. Chem. Sci.*, 2006, **118**, 319.

11 The complex **4** appears to show dynamic behaviour around room temperature in solution. This might be due to the metal–metal bond cleavage process or the migration of the hydrides between the metal centers, though the detail is not clear.

12 We have observed that no reaction of the monometallic complex **1** with alkynes (methyl propiolate and phenylacetylene) occur, indicating that the dimetallic cores are essential for the alkyne insertion reaction.

13 We have also examined the reactions of **3** with internal alkynes (diphenylacetylene and dimethyl acetylenedicarboxylate), however, no reaction takes place.

14 Similar large vicinal ^{31}P–^{1}H coupling constants in P–O–C–H have been reported. W. Kung, R. E. Marsh and M. Kainosho, *J. Am. Chem. Soc.*, 1977, **99**, 5471.

15 We could not isolate and characterize the minor product.

16 Heating a solution of pure **9** gave a mixture of **9** and **10**, though the formation of the type **I′**, **III**, or **III′** isomer was not observed.

17 It has been reported that the π-coordination of a carbon–carbon triple bond to a metal center bound to a phosphorus ligand is more predominant compared to that to a metal center bound to a pyridine ligand: C. Dubs, T. Yamamoto, A. Inagaki and M. Akita, *Organometallics*, 2006, **25**, 1359.

18 We have also carried out the reaction of **3** with phenylacetylene-d_1, which resulted in the formation of **9**-d_1 having a deuterium at the *trans* β-vinyl position (> 90% D).

19 Coordination of an alkyne to iridium center in a hetero-dimetallic (Ir–Rh) complex has been reported: B. A. Vaartstra and M. Cowie, *Organometallics*, 1989, **8**, 2388.

20 Theoretical thermochemical analysis of hydrometallation of a carbon–carbon unsaturated bond by CpIr and CpRh complexes has been reported: Y. Han, L. Deng and T. Ziegler, *J. Am. Chem. Soc.*, 1997, **119**, 5939.

21 Rotational isomerization of an η^1,η^2-alkenyl ligand on a monometallic complex has been reported: J. L. Davidson, W. F. Wilson, L. Manojlović-Muir and K. W. Muir, *J. Organomet. Chem.*, 1983, **254**, C6.

22 (*a*) J. R. Shapley, S. I. Richter, M. Tachikawa and J. B. Keister, *J. Organomet. Chem.*, 1975, **94**, C43; (*b*) A. D. Clauss, M. Tachikawa, J. R. Shapley and C. G. Pierpont, *Inorg. Chem.*, 1981, **20**, 1528; (*c*) P. O. Nubel and T. L. Brown, *J. Am. Chem. Soc.*, 1984, **106**, 3474; (*d*) L. J. Farrugia, Y. Chi and W.-C. Tu, *Organometallics*, 1993, **12**, 1616.

23 This species rapidly converted into **14b** at room temperature. NMR data of the detected species: ^{1}H NMR δ/ppm: 4.90 (dd, $J_{PH} = 2$ Hz, $J_{HH} = 2$ Hz, μ-vinyl proton), 0.71 (d, $J_{HH} = 2$ Hz, μ-vinyl proton). $^{13}C\{^{1}H\}$ NMR δ/ppm: 120.7 (d, $J = 8$ Hz, C^{α}), 70.9 (d, $J = 7$ Hz, C^{β}). $^{31}P\{^{1}H\}$ NMR δ/ppm: 34.9 (s). The structure of this species might be the type **I**, **I′**, or **III**. We wish to characterize this species in due course.

24 The isomerization of the type **I** complexes into the type **III′** complexes would be ascribed to the differences in bond energies between the metal–carbon σ-bond in the type **I** and the iridium–carbon σ-bond in the type **III′**. Generally, iridium–carbon bonds are most stable, and rhodium–carbon bonds are more stable than ruthenium–carbon bonds. Accordingly, the isomerization of **7** did not occur, the isomerization of **12a** to **12b** slowly proceeded, and the isomerization to **14b** would be very rapid. As to the metal–carbon bond strengths, see: J. A. M. Simões and J. L. Beauchamp, *Chem. Rev.*, 1990, **90**, 629.

25 C. White, A. Yates and P. M. Maitlis, *Inorg. Synth.*, 1992, **29**, 228.

26 P. J. Fagan, M. D. Ward and J. C. Calabrese, *J. Am. Chem. Soc.*, 1989, **111**, 1698.

27 P. T. Beurskens, G. Admiraal, G. Beurskens, W. P. Bosman, S. Garcia-Granda, R. O. Gould, J. M. M. Smits and C. Smykalla, *The DIRDIF program system*, Technical Report of the Crystallography Laboratory, University of Nijmegen, Nijmegen, The Netherlands, 1992.

28 P. T. Beurskens, G. Admiraal, G. Beurskens, W. P. Bosman, R. de Gelder, R. Israel and J. M. M. Smits, *The DIRDIF-99 program system*, Technical Report of the Crystallography LaboratoryUniversity of Nijmegen, Nijmegen, The Netherlands, 1999.

29 A. Altomare, G. Cascarano, C. Giacovazzo, A. Guagliardi, M. Burla, G. Polidori and M. Camalli, *J. Appl. Crystallogr.*, 1994, **27**, 435.

30 (*a*) D. T. Cromer, and G. T. Waber, *International Table for X-Ray Crystallography*, The Kynoch Press, Birmingham, U.K., 1974; vol. IV, table 2.2 A; (*b*) J. A. Ibers and W. C. Hamilton, *Acta Crystallogr.*, 1964, **17**, 871; (*c*) D. C. Creagh, and W. J. McAuley, in *International Tables for X-Ray Crystallography*, ed. A. J. C. Wilson, Kluwer Academic Publishers, Boston, 1992; vol. C, pp. 219–222, table 4.2.6.8; (*d*) D. C. Creagh, and J. H. Hubbell, in *International Tables for X-Ray Crystallography*, ed. A. J. C. Wilson, Kluwer Academic Publishers, Boston, 1992; vol. C, pp. 200–206, table 4.2.4.3.

31 *CrystalStructure3.8*, Crystal Structure Analysis Package, Rigaku and Rigaku/Molecular Structure Corp., 2000–2006.

32 J. R. Carruthers, J. S. Rollett, P. W. Betteridge, D. Kinna, L. Pearce, A. Larsen and E. Gabe, *CRYSTALS Issue 11*, Chemical Crystallography Laboratory, Oxford, 1999.

